6

Forced Convection Mass-Transfer Enhancement in Mixing Systems

Rafał Rakoczy and Stanisław Masiuk
Institute of Chemical Engineering and Environmental Protection Process,
West Pomeranian University of Technology
al. Piastów 42, 71-065 Szczecin
Poland

1. Introduction

The design, scale-up and optimization of industrial processes conducted in agitated systems require, among other, precise knowledge of the hydrodynamics, mass and heat transfer parameters and reaction kinetics. Literature data available indicate that the mass-transfer process is generally the rate-limiting step in many industrial applications. Because of the tremendous importance of mass-transfer in engineering practice, a very large number of studies have determined mass-transfer coefficients both empirically and theoretically.
Agitated vessels find their use in a considerable number of mass-transfer operations. They are usually employed to dissolve granular or powdered solids into a liquid solvent in preparation for a reaction of other subsequent operations (Basmadjian, 2004). Agitation is commonly used in leaching operations or process of precipitation, crystallization and liquid extraction.
Transfer of the solute into the main body of the fluid occurs in the three ways, dependent upon the conditions. For an infinite stagnant fluid, transfer will be by the molecular diffusion augmented by the gradients of temperature and pressure. The natural convection currents are set up owing to the difference in density between the pure solvent and the solution. This difference in inducted flow helps to carry solute away from the interface. The third mode of transport is depended on the external effects. In this way, the forced convection closely resembles natural convection expect that the liquid flow is involved by using the external force.
Mass-transfer process in the mixing systems is very complicated and may be described by the non-dimensional Sherwood number, as a rule is a function of the Schmidt number and the dimensionless numbers describing the influence of hydrodynamic conditions on the realized process. In chemical engineering operations the experimental investigations are usually concerned with establishing the mass-transfer coefficients that define the rate of transport to the continuous phase.
One of the key aspects in the dynamic behaviour of the mass-transfer processes is the role of hydrodynamics. On a macroscopic scale, the improvement of hydrodynamic conditions can be achieved by using various techniques of mixing, vibration, rotation, pulsation and oscillation in addition to other techniques like the use of fluidization, turbulence promotes or magnetic and electric fields etc.

In this work, the focus is on a mass-transfer process under various types of augmentation technique, i.e.: rotational and reciprocating mixers, and rotating magnetic field. According to the information available in technical literature, the review of the empirical equations useful to generalize the experimental data for various types of mixers is presented. Moreover, the usage of static, rotating and alternating magnetic field to augment the mass process intensity instead of mechanically mixing is theoretical and practical analyzed.

2. Problem formulation of mass diffusion under the action of forced convection

Under forced convective conditions, the mathematical description of the solid dissolution process may be described by means of the integral equation of mass balance for the component *i*, namely,

$$\int_V \frac{\partial \rho_i}{\partial \tau} dV = -\int_S \rho_i \cdot \left(\overline{w_i} \cdot \overline{n}\right) dS + \int_V j_i \, dV \tag{1}$$

where: j_i - volumetric mass source of component *i*, $kg_i \cdot m^3 \cdot s^{-1}$; $\overline{n}$ - normal component; $\overline{w_i}$ - vector velocity of component *i*, $m \cdot s^{-1}$; S - area, m^2; V - volume, m^3; ρ_i - concentration of component *i*, $kg_i \cdot m^{-3}$; τ - time, s.

The above equation (1) for homogenous mixture may be written in the following differential form

$$\frac{\partial \rho_i}{\partial \tau} + div\left(\rho_i \overline{w_i}\right) = j_i \tag{2}$$

The vector velocity of component *i*, $\overline{w_i}$, can be defined by using the averaged value of momentum, $([\overline{q}_i]_{avg})$

$$\overline{w_i} = \lim_{V \to 0} \frac{\left[\overline{q_i}\right]_{avg}}{m_i} \tag{3}$$

The velocity of component *i*, $\overline{w_i}$, in relation to the velocity of mixture or liquid, $\overline{w}$, is defined as follows

$$dif\,\overline{w_i} = \overline{w_i} - \overline{w} \Rightarrow dif\,\overline{w_i} = \overline{w_i} - \frac{1}{\rho}\sum_i \rho_i \overline{w_i} \tag{4}$$

Introducing the relation (4) in equation (2), gives the following relationship for the mass balance of *i* component

$$\frac{\partial \rho_i}{\partial \tau} + div\left[\rho_i \left(dif\,\overline{w_i} + \overline{w_i}\right)\right] = j_i \tag{5}$$

The above equation (5) can be rewritten as follows

$$\frac{\partial \rho_i}{\partial \tau} + div\left(\rho_i \overline{w}\right) = -div\left(\overline{j_i}\right) + j_i \tag{6}$$

The mass concentration of component *i*, c_i, may be defined in the following form

$$c_i = \frac{\rho_i}{\rho} \Rightarrow \rho_i = \rho c_i \tag{7}$$

Then, the differential equation of mass balance (equation 6) for the mass concentration of component *i*, c_i, may be given by:

$$\rho \frac{dc_i}{d\tau} + div\left(\overline{j_i}\right) - j_i = 0 \tag{8}$$

The term $\left(\rho \frac{dc_i}{d\tau}\right)$ in the above equation (8) expresses the local accumulation of relative mass and the convectional mass flow rate of component *i*, whereas the term $\overline{j_i}$ is total diffusion flux density of component *i*. The term (j_i) describes the intensity of the process generation of the volumetric mass flux of component *i* in the volume *V* due to the dissolution process. The resulting diffusion flux is expressed as a sum of elementary fluxes considering the concentration (*c*), temperature (*T*), thermodynamic pressure gradient (*p*), and the additional force interactions ($\overline{F}$) (i.e. forced convection as a result of fluid mixing) in the following form

$$\overline{j_i} = \overline{j_i}(c) + \overline{j_i}(T) + \overline{j_i}(p) + \overline{j_i}\left(\overline{F}\right) \tag{9}$$

A more useful form of this equation may be obtained by introducing the proper coefficients as follows

$$\overline{j_i} = -\rho D_i \, grad(c_i) - \rho D_i k_T \, grad(\ln T) - \rho D_i k_p \, grad(\ln p) - \rho D_i k_{\overline{F}} \, \overline{F} \tag{10}$$

where: D_i - coefficient of molecular diffusion, $m^2 \cdot s^{-1}$; k_T - relative coefficient of thermodiffusion, $kg_i \cdot kg^{-1}$; k_p - relative coefficient of barodiffusion, $kg_i \cdot kg^{-1}$; $k_{\overline{F}}$ - relative coefficient of forced diffusion, $kg_i \cdot m^2 \cdot kg^{-1} \cdot N^{-1}$.

In the case of the experimental investigations of mass-transfer process from solid body to its flowing surrounding dilute solution, the boundary layer around the sample is generated. This layer is dispersed in the agitated volume by means of the physical diffusion process and the diffusion due to the forced convection. Then, the differential equation of mass balance equation for the mass concentration of component *i* diffuses to the surrounding liquid phase is given as follows

$$\frac{\partial c_i}{\partial \tau} + \overline{w} \, grad \, c_i + div\left(\frac{\overline{j_i}}{\rho}\right) = \frac{j_i}{\rho} \tag{11}$$

Introducing relation (10) in the equation (11) gives the following relationship for the balance of the mass concentration of component *i* where force $\overline{F}$ is generated by the mixing process

$$\frac{\partial c_i}{\partial \tau} + \overline{w} \, grad \, c_i + div\left[-D_i \, grad \, c_i - a\left(\frac{\partial c_i}{\partial T}\right)_{\substack{p=const \\ p_{\overline{F}}=const}} grad \, T - \nu \left(\frac{\partial c_i}{\partial p}\right)_{\substack{T=const \\ p_{\overline{F}}=const}} grad \, p \right] + div\left(\frac{\overline{F}}{\dot{G}} c_i\right) = \frac{j_i}{\rho} \tag{12}$$

where: ν - kinematic viscosity, m²·s⁻¹; $\dot{G}$ - mass flow rate, kg·s⁻¹.
The above relation (12) may be treated as the differential mathematical model of the dissolution process of solid body. The right side of the above equation (12) represents the source mass flux of component *i*. This expression may be represented by the differential kinetic equation for the dissolution of solid body as follows

$$
\begin{aligned}
&-\frac{dm_i(\tau)}{d\tau} = \beta_i dF_s(\tau)\frac{dc_i(\tau)}{d\tau}d\tau \Rightarrow -\frac{d\rho_i(\tau)}{d\tau} = \beta_i \frac{dF_s(\tau)}{dV_s(\tau)}\frac{dc_i(\tau)}{d\tau}d\tau \Rightarrow \\
&\Rightarrow -\frac{d\rho_i(\tau)}{d\tau} = \beta_i \frac{dc_i(\tau)}{dr\,d\tau}d\tau \Rightarrow \frac{d\rho_i(\tau)}{d\tau} = \beta_i\left(grad\,c_i(\tau)\overline{e_r}\right) \Rightarrow \\
&\Rightarrow \beta_i = \frac{d\rho_i(\tau)}{\left(grad\,c_i(\tau)\overline{e_r}\right)d\tau}
\end{aligned}
\tag{13}
$$

where: β_i - mass-transfer coefficient in a mixing process, kg·m⁻²·s⁻¹; m_i - mass of dissolving solid body, kg$_i$; F_s - surface of dissoluble sample, m².
The above equation (13) cannot be integrated because the area of solid body, F_s, is changing in time of dissolving process. It should be noted that the change in mass of solid body in a short time period of dissolving is very small and the mean area of dissolved cylinder may be used. The relation between loss of mass, mean area of mass-transfer and the mean driving force of this process for the time of dissolving duration is approximately linear and then the mass-transfer coefficient may be calculated from the simple linear equation

$$
\left[\beta_i\right]_{avg} = \frac{\Delta m_i}{\left[F_s\right]_{avg}\Delta c_i \Delta\tau} \tag{14}
$$

Taking into account the above relations (equations 13 and 14) we obtain the following general relationship for the mass balance of component *i*

$$
\begin{aligned}
&\frac{\partial c_i}{\partial\tau} + \overline{w}\,grad\,c_i + div\left[-D_i\,grad\,c_i - a\left(\frac{\partial c_i}{\partial T}\right)_{\substack{p=const\\ p_{\overline{F}}=const}} grad T - \nu\left(\frac{\partial c_i}{\partial p}\right)_{\substack{T=const\\ p_{\overline{F}}=const}} grad\,p\right] + \\
&+div\left(\frac{\overline{F}}{\dot{G}}c_i\right) = \frac{\left[\beta_i\right]_{avg}\left(grad\,c_i\right)\overline{e_r}}{\rho}
\end{aligned}
\tag{15}
$$

The obtained equation (15) suggests that this dependence may be simplified in the following form:

$$
\frac{\partial c_i}{\partial\tau} + \overline{w}\,grad\,c_i - div\left(D_i\,grad\,c_i\right) + div\left(\frac{\overline{F}}{\dot{G}}c_i\right) = \frac{\left[\beta_i\right]_{avg}\left(grad\,c_i\right)\overline{e_r}}{\rho} \tag{16}
$$

The agitated vessels find their use in a considerable number of mass-transfer operations. Practically, the intensification of the mass-transfer processes may be carried out by means of the vertical tubular cylindrical vessels equipped with the rotational (Nienow et al., 1997) or the reciprocating agitators (Masiuk, 2001). Under forced convective conditions, the force $\overline{F}$ in equation (16) may be defined (Masiuk, et al. 2008):

- for rotational agitator $$\overline{F_{rot}} = \rho V \frac{d\overline{w_{rot}}}{dt} \Rightarrow \overline{F_{rot}} = \rho V 2\pi^2 n^2 d_{rot} \overline{e_\varphi} \tag{17}$$

- for reciprocating agitator $$\overline{F_{rec}} = \rho V \frac{d\overline{w_{rec}}}{dt} \Rightarrow \overline{F_{rec}} = \rho V 4\pi^2 A f^2 \overline{e_z} \tag{18}$$

where: A - amplitude of reciprocating agitator, m; d_{rec} - diameter of reciprocating agitator, m; d_{rot} - diameter of rotational agitator, m; f - frequency of reciprocating agitator, s^{-1}; n - rotational speed of agitator, s^{-1}; V - liquid volume, $kg \cdot m^{-3}$; ρ - liquid density, $kg \cdot m^{-3}$.
Introducing the proposed relationships (17) and (18) in equation (16), give the following relations for the agitated system by using the rotational and reciprocating agitator, respectively

$$\frac{\partial c_i}{\partial \tau} + \overline{w}\, grad\, c_i - div\left(D_i\, grad\, c_i\right) + div\left(\frac{\rho V n^2 d_{rot}}{\dot{G}_{rot}} c_i \overline{e_\varphi}\right) = \frac{\left[\beta_i\right]_{avg} \left(grad\, c_i\right) \overline{e_r}}{\rho} \tag{19}$$

$$\frac{\partial c_i}{\partial \tau} + \overline{w}\, grad\, c_i - div\left(D_i\, grad\, c_i\right) + div\left(\frac{\rho V A f^2}{\dot{G}_{rec}} c_i \overline{e_z}\right) = \frac{\left[\beta_i\right]_{avg} \left(grad\, c_i\right) \overline{e_r}}{\rho} \tag{20}$$

The mass flow rate for the rotational and the reciprocating agitator can be approximated by the following equations:

$$\dot{G}_{rot} = \rho V n \tag{21}$$

$$\dot{G}_{rec} = \rho V f \tag{22}$$

Taking into consideration the above relations (equations 21 and 22), we obtain the following relationships:

$$\frac{\partial c_i}{\partial \tau} + \overline{w}\, grad\, c_i - div\left(D_i\, grad\, c_i\right) + div\left(n d_{rot} c_i \overline{e_\varphi}\right) = \frac{\left[\beta_i\right]_{avg} \left(grad\, c_i\right) \overline{e_r}}{\rho} \tag{23}$$

$$\frac{\partial c_i}{\partial \tau} + \overline{w}\, grad\, c_i - div\left(D_i\, grad\, c_i\right) + div\left(A f c_i \overline{e_z}\right) = \frac{\left[\beta_i\right]_{avg} \left(grad\, c_i\right) \overline{e_r}}{\rho} \tag{24}$$

2.1 Definition of dimensionless numbers for mass-transfer process

The governing equations (23) and (24) may be rewritten in a symbolic shape which is useful for the dimensionless analysis. The introduction of the non-dimensional quantities denoted by sign $(^*)$ into these relationships yield:

$$\begin{aligned} &\frac{c_{i_0}}{\tau_0}\left[\frac{\partial c_i^*}{\partial \tau^*}\right] + \frac{w_0 c_{i_0}}{l_0}\left[\overline{w}^*\, grad\, c_i\right] - \frac{D_{i_0} c_{i_0}}{l_0^2}\left[div^*\left(D_i^*\, grad^* c_i^*\right)\right] + \\ &+ \frac{n_0 d_{rot_0} c_{i_0}}{l_0}\left[div^*\left(n^* d_{rot}^* c_i^* \overline{e_\varphi}\right)\right] = \frac{\left[\beta_i\right]_{avg_0} c_{i_0}}{l_0 \rho_0}\left[\frac{\left[\beta_i\right]_{avg}^* \left(grad^* c_i^*\right) \overline{e_r}}{\rho^*}\right] \end{aligned} \tag{25}$$

$$\frac{c_{i_0}}{\tau_0}\left[\frac{\partial c_i^*}{\partial \tau^*}\right]+\frac{w_0 c_{i_0}}{l_0}\left[\overline{w}^*\ grad\, c_i\right]-\frac{D_{i_0} c_{i_0}}{l_0^2}\left[div^*\left(D_i^*\ grad^* c_i^*\right)\right]+$$
$$+\frac{A_0 f_0 c_{i_0}}{l_0}\left[div^*\left(A^* f^* c_i^* \overline{e}_z\right)\right]=\frac{[\beta_i]_{avg_0} c_{i_0}}{l_0 \rho_0}\left[\frac{[\beta_i]_{avg}^*\left(grad^* c_i^*\right)\overline{e}_r}{\rho^*}\right] \tag{26}$$

The non-dimensional forms of these equations may be scaled against the convective term $\left(\frac{w_0 c_{i_0}}{l_0}\right)$. The dimensionless forms of the equations (25) and (26) may be given as follows:

$$\frac{l_0}{\tau_0 w_0}\left[\frac{\partial c_i^*}{\partial \tau^*}\right]+\left[\overline{w}^*\ grad\, c_i\right]-\frac{D_{i_0}}{l_0 w_0}\left[div^*\left(D_i^*\ grad^* c_i^*\right)\right]+$$
$$+\frac{n_0 d_{rot_0}}{w_0}\left[div^*\left(n^* d_{rot}^* c_i^* \overline{e}_\varphi\right)\right]=\frac{[\beta_i]_{avg_0}}{\rho_0 w_0}\left[\frac{[\beta_i]_{avg}^*\left(grad^* c_i^*\right)\overline{e}_r}{\rho^*}\right] \tag{27}$$

$$\frac{l_0}{\tau_0 w_0}\left[\frac{\partial c_i^*}{\partial \tau^*}\right]+\left[\overline{w}^*\ grad\, c_i\right]-\frac{D_{i_0}}{l_0 w_0}\left[div^*\left(D_i^*\ grad^* c_i^*\right)\right]+$$
$$+\frac{A_0 f_0}{w_0}\left[div^*\left(A^* f^* c_i^* \overline{e}_z\right)\right]=\frac{[\beta_i]_{avg_0}}{\rho_0 w_0}\left[\frac{[\beta_i]_{avg}^*\left(grad^* c_i^*\right)\overline{e}_r}{\rho^*}\right] \tag{28}$$

The equations (27) and (28) include the following dimensionless groups characterising the mass-transfer process under the action of the rotational or the reciprocating agitator:

$$\frac{l_0}{\tau_0 w_0} \Rightarrow \frac{D}{\tau_0 n_0 d_{rot_0}} \Rightarrow S_{rot}^{-1} \tag{29a}$$

$$\frac{l_0}{\tau_0 w_0} \Rightarrow \frac{D}{\tau_0 A_0 f_0} \Rightarrow S_{rec}^{-1} \tag{29b}$$

$$\frac{D_{i_0}}{l_0 w_0} \Rightarrow \left(\frac{\nu}{l_0 w_0}\right)\left(\frac{D_{i_0}}{\nu}\right) \Rightarrow \left(\frac{\nu}{w_0 D}\right)\left(\frac{D_{i_0}}{\nu}\right) \Rightarrow Re^{-1}\, Sc^{-1} \Rightarrow Pe_{mass}^{-1} \tag{30}$$

$$\frac{n_0 d_{rot_0}}{w_0} \Rightarrow \left(\frac{n_0 d_{rot_0}}{n_0 d_{rot_0}}\right) \Rightarrow 1 \tag{31a}$$

$$\frac{A_0 f_0}{w_0} \Rightarrow \left(\frac{A_0 f_0}{A_0 f_0}\right) \Rightarrow 1 \tag{31b}$$

$$\frac{[\beta_i]_{avg_0}}{\rho_0 w_0} \Rightarrow \left(\frac{[\beta_i]_{avg_0} d_s}{\rho_0 D_i}\right)\left(\frac{\nu}{w_0 d_{rot}}\right)\left(\frac{D_i}{\nu}\right)\left(\frac{d_{rot}}{d_s}\right) \Rightarrow$$
$$\Rightarrow \left(\frac{[\beta_i]_{avg_0} d_s}{\rho_0 D_i}\right)\left(\frac{\nu}{n d_{rot}^2}\right)\left(\frac{D_i}{\nu}\right)\left(\frac{d_{rot}}{d_s}\right) \Rightarrow Sh\, Re_{rot}^{-1} Sc^{-1}\left(\frac{d_{rot}}{d_s}\right) \quad (32a)$$

$$\frac{[\beta_i]_{avg_0}}{\rho_0 w_0} \Rightarrow \left(\frac{[\beta_i]_{avg_0} d_s}{\rho_0 D_i}\right)\left(\frac{\nu}{w_0 d_{rec}}\right)\left(\frac{D_i}{\nu}\right)\left(\frac{d_{rec}}{d_s}\right) \Rightarrow$$
$$\Rightarrow \left(\frac{[\beta_i]_{avg_0} d_s}{\rho_0 D_i}\right)\left(\frac{\nu}{A_0 f_0 d_{rec}}\right)\left(\frac{D_i}{\nu}\right)\left(\frac{d_{rec}}{d_s}\right) \Rightarrow Sh\, Re_{rec}^{-1} Sc^{-1}\left(\frac{d_{rec}}{d_s}\right) \quad (32b)$$

where: D - diameter of vessel, m.

Taking into account the proposed relations (29-32), we find the following dimensionless governing equations:

- for rotational agitator

$$S_{rot}^{-1}\left[\frac{\partial c_i^*}{\partial \tau^*}\right] + \left[\overline{w}^*\, grad\, c_i\right] - Pe_{mass}^{-1}\left[div^*\left(D_i^*\, grad^* c_i^*\right)\right] + \left[div^*\left(n^* d_{rot}^* c_i^* \overline{e_\varphi}\right)\right] = Sh\, Re_{rot}^{-1} Sc^{-1}\left(\frac{d_{rot}}{d_s}\right)\left[\frac{[\beta_i]_{avg}^*\left(grad^* c_i^*\right)\overline{e_r}}{\rho^*}\right] \quad (33)$$

Name	Symbol	Definition	Significance	Interpretation and Remarks
Strouhal	S	$\frac{\tau_0 w_0}{D}$	$\frac{convection}{unsteadiness}$	Dimensionless number describing oscillating flow mechanism
Péclet (mass)	Pe_{mass}	$\frac{w_0 D}{D_i}$	$\frac{hydrodynamic\ convection}{mass\ diffusion}$	Dimensionless independent mass-transfer parameter. $Pe_{mass} = Re\, Sc$
Reynolds (rot)	Re_{rot}	$\frac{n_0 d_{rot_0}^2}{\nu_0}$	$\frac{interial\ force\ /\ convection}{viscous\ force}$	Reynolds number for the rotational agitator.
Reynolds (rec)	Re_{rec}	$\frac{A_0 f_0 d_{rec}}{\nu_0}$		Reynolds number for the reciprocating agitator.
Sherwood	Sh	$\frac{[\beta_i]_{avg} d_s}{\rho_0 D_i}$	$\frac{convective\ mass\ transport}{diffusive\ mass\ transport}$	mass-transfer Stanton number $St_m = Sh\, Sc^{-1}\, Re^{-1}$
Schmidt	Sc	$\frac{\nu_0}{D_i}$	$\frac{momentum\ diffusion}{molecular\ diffusion}$	$Sc = Re^{-1}\, Pe_{mass}$

Table 1. Dimensionless parameters in equations (33) and (34) and their physical role

-for reciprocating agitator

$$S_{rec}^{-1}\left[\frac{\partial c_i^*}{\partial \tau^*}\right]+\left[\overline{w}^*\ grad\, c_i\right]-Pe_{mass}^{-1}\left[div^*\left(D_i^*\ grad^* c_i^*\right)\right]+ \\ +\left[div^*\left(A^* f^* c_i^* \overline{e}_z\right)\right]=Sh\, Re_{rec}^{-1} Sc^{-1}\left(\frac{d_{rec}}{d_s}\right)\left[\frac{\left[\beta_i\right]_{avg}^*\left(grad^* c_i^*\right)\overline{e}_r}{\rho^*}\right] \quad (34)$$

Table 1 summarizes all essential and independent dimensionless parameters met in mass-transfer process under the action of the agitated systems.

From dimensionless form of equation (34) and (35) it follows that:

- for rotational agitator $$Sh\, Re_{rot}^{-1} Sc^{-1}\left(\frac{d_{rot}}{d_s}\right)\sim 1 \Rightarrow Sh \sim Re_{rot}\, Sc\, \left(\frac{d_s}{d_{rot}}\right) \quad (35)$$

- for reciprocating agitator $$Sh\, Re_{rec}^{-1} Sc^{-1}\left(\frac{d_{rec}}{d_s}\right)\sim 1 \Rightarrow Sh \sim Re_{rec}\, Sc\, \left(\frac{d_s}{d_{rec}}\right) \quad (36)$$

2.2 Mass-transfer characteristics

Under convective conditions a relationship for the mass-transfer similar to the relationships obtained for heat-transfer may be expected of the form (Incropera & DeWitt, 1996):

$$Sh = f\left(Re, Sc\right) \quad (37)$$

The two principle dimensionless groups of relevance to mass-transfer are Sherwood and Schmidt numbers. The Sherwood number can be viewed as describing the ratio of convective to diffusive transport, and finds its counterpart in heat transfer in the form of the Nusselt number (Basmadjian, 2004).

The Schmidt number is a ratio of physical parameters pertinent to the system. This dimensionless group corresponds to the Prandtl number used in heat-transfer. Moreover, this number provides a measure of the relative effectiveness of momentum and mass transport by diffusion.

Added to these two groups is the Reynolds number, which represents the ratio of convective-to-viscous momentum transport. This number determines the existence of laminar or turbulent conditions of fluid flow. For small values of the Reynolds number, viscous forces are sufficiently large relative to inertia forces. But, with increasing the Reynolds number, viscous effects become progressively less important relative to inertia effects.

Two additional dimensionless groups, the Péclet number and the Stanton number (see Table 1) are also used and they are composed of other non-dimensional groups.

Evidently, for relation (37) to be of practical use, it must be rendered quantitative. This may be done by assuming that the functional relation is in the following form (Kay & Crawford, 1980)

$$Sh = a\, Re^b\, Sc^c \quad (38)$$

The mass-transfer coefficients in the agitated systems can be correlated by the combination of Sherwood, Reynolds and Schmidt numbers. Using the proposed relation (38), it has been

found possible to correlate a host of experimental data for a wide range of operations. The coefficients of relation (38) are determined from experiment.
For mass-transfer under natural-convection conditions, where the Reynolds number is unimportant, the mass-transfer may be described by using the following general expression (Bird et al., 1966)

$$Sh = f\left(Gr, Sc\right) \tag{39}$$

The Grashof number, Gr, plays the same role in free convection that the Reynolds number plays in forced convection. Recall that the Reynolds number provides a measure of the ratio of the inertial to viscous forces acting on a fluid element. In contrast, the Grashof number indicates the ratio of the buoyancy force to the viscous force acting on the fluid (Fox & McDonald, 1993).
Under forced convection conditions where the Grashof number is unimportant the boundary layer theory suggests the following form of the relation (38) (Garner & Suckling, 1958)

$$Sh = 0.023 Re^{0.83} Sc^{0.44} \tag{40}$$

The exponent upon of the Schmidt number is to be 0.33 (Noordsij & Rotte, 1968; Jameson, 1964; Condoret et al., 1989; Tojo et al., 1981; Lemcoff & Jameson, 1975) as there is some theoretical and experimental evidence for this value (Sugano & Rutkowsky, 1968), although reported values vary from 0.56 (Wong et al., 1978) to 1.13 (Lemlich & Levy, 1961).
A dimensionless group often used in literature is the Colburn factor j for mass transfer, which is defines as follows (Geankoplis, 2003)

$$j_m = St_m Sc^{0.66} \tag{41}$$

3. Mass-transfer correlations in rotationally agitated liquid-solid systems

We have compiled a list of the most frequently used correlations and tabulated them in Table 2. The following correlations have been found useful in predicting transport coefficients in the agitated systems. These equations may be successfully applied to analyze the case of the dissolution of solid bodies in a stirred tank.
As it mentioned above, mass-transfer process is very complicated and may be described by the non-dimensional Sherwood number, as a rule is a function of the Schmidt number and the dimensionless numbers describing the influence of hydrodynamic conditions on the realized process. Use of the dimensionless Sherwood number as a function of the various non-dimensional parameters (see relation 37 or 39) yields a description of liquid-side mass-transfer, which is more general and useful. In majority of the works, both theoretical and practical (see Table 2), the correlations of mass-transfer process have the general form

$$Sh = 2 + aRe^{b} Sc^{c} \tag{42}$$

where the Sherwood number is a function of the Reynolds number, the Schmidt number, and differ by the fitting parameters *a, b* and *c*.

References	Correlation	Situation	Comments
(Hixon & Baum, 1941)	$Sh = 0.16\, Re^{0.62}\, Sc^{0.5}$	Solid-liquid agitated systems (turbine agitator with inclined blades)	$Re > 6.7 \cdot 10^4$
(Hixon & Baum, 1944)	$Sh = 2.7 \cdot 10^{-5}\, Re^{1.4}\, Sc^{0.5}$		$Re < 6.7 \cdot 10^4$
(Hixon & Baum, 1942)	$Sh = 3.5 \cdot 10^{-5}\, Re^{1.0}\, Sc^{0.5}$	Solid-liquid agitated systems (propeller agitator)	$Re = 3 \cdot 10^4 - 5 \cdot 10^6$
(Humphrey & Van Ness, 1957)	$Sh = 0.58\, Re^{0.58}\, Sc^{0.5}$	Solid-liquid agitated systems (propeller agitator, baffles)	$Re = 6.3 \cdot 10^3 - 3.3 \cdot 10^5$
	$Sh = 0.022\, Re^{0.87}\, Sc^{0.5}$	Solid-liquid agitated systems (turbine agitator, baffles)	$Re = 3.1 \cdot 10^4 - 9 \cdot 10^4$
(Barker & Treybal, 1960)	$Sh = 0.052\, Re^{0.833}\, Sc^{0.5}$	Solid-liquid agitated systems (turbine agitator, baffles)	$Re = 3.1 \cdot 10^3 - 3 \cdot 10^5$
(Harriot, 1962)	$Sh = 2 + 0.6\, Re^{0.5}\, Sc^{0.33}$	Solid particles suspended in agitated vessel with baffles	$Re = \frac{v_{slip} d_p}{\nu} \Rightarrow Re = \frac{v_T d_p}{\nu}$
(Weinspach 1967)	$Sh = 10.68 \cdot 10^2\, Re^{0.15}\, Sc^{0.08} \left(\frac{d_s}{d}\right)^{1.15}$	Correlation for various types of agitators and mixer with baffles	$Re \rightarrow$ turbulent region
	$Sh = 7.2 \cdot 10^{-2}\, Ar^{0.33}\, Sc^{0.56} \left(\frac{d_s}{d}\right)$		$Ar = \frac{d^3 g \Delta\rho \rho_c}{\eta_c^2}$ $Ar\left(\frac{d_s}{d}\right) = 10^2 - 10^7; Sc = 10^2 - 10^5$
(Levins & Gastonbury, 1972)	$Sh = 2 + 0.44\, Re^{0.5}\, Sc^{0.38}$	Solid particles with significant density difference	$Re = \frac{v_{slip} d_p}{\nu}$

Table 2. Summary of mass-transfer correlations for agitated systems

References	Correlation	Situation	Comments
(Liepe & Möckel, 1976)	$Sh = 2 + 0.67 Re_{\varepsilon}^{3/8} Sc^{1/3}$	Solid-liquid agitated systems	$d_s < d_{s,\lim}$ $d_{s,\lim} = 5.2\left(\frac{\Delta\rho}{\rho}\right)^{-5/6}\left(\frac{\nu_c^3}{\langle\bar{\varepsilon}\rangle}\right)^{1/4}$ d_s - size of solid grain, m
	$Sh = 2 + 0.35 Re_{\varepsilon}^{2}\left(\frac{\Delta\rho}{\rho}\right)^{1/3}$		$d_s > d_{s,\lim}$
(Herndl & Mersmann, 1982)	$Sh = 2 + 0.46 Re_{\varepsilon}^{2/3} Sc^{1/3}$	Solid-liquid agitated systems	$Re_{\varepsilon} = \left(\frac{d_s^4 \langle\bar{\varepsilon}\rangle}{\nu_c^3}\right)^{1/3}$;$1 < Re_{\varepsilon} < 10^3$ ε - energy dissipation rate, W·kg1
(Kirwan, 1987)	$Sh = 2 + 0.52\, Re^{0.52}\, Sc^{0.33}$	Small solid particles	$Re = \frac{E^{1/3} d_p^{4/3}}{\nu} < 1.0$
(Ditl et al., 1991)	$Sh = 2 + 0.43 Re_{\varepsilon}^{0.6} Sc^{0.39}\left(\frac{D}{d}\right)^{-0.25}$	Solid-liquid agitated systems	-
(Basmadjian, 2004)	$Sh = 1.46\, Re^{0.65}\, Sc^{0.33}$	Solid-liquid baffled vessel $Re = 10^4 - 10^6$	$Sh = \frac{k_c d_v}{D_i}$; $Re = \frac{d_i^2 n}{\nu}$ k_c - mass transfer coefficient, m2·s-1 $d_i n$ - dimensional velocity, where n - represents the number revolutions per unit time, m·s-1
(Hartmann et al. 2006)	$Sh = 2 + 0.6\, Re_p^{0.5}\, Sc^{0.33}$	Solid particles suspended in liquid	$Re_p = \frac{v_T d_p}{\nu}$ Re_p - particle Reynolds number

Table 2. Summary of mass-transfer correlations for agitated systems-continuation

Instead of Reynolds number, it would be more natural to express the Sherwood number in terms of the Pèclet number, which is the product of the Reynolds and Schmidt numbers (see Table 2). When this number is small, transport takes place due to mass diffusion, and the fluid velocity, density and viscosity do not affect the transport rates. In this case, the Sherwood number is a constant, dependent only on the configuration. For laminar flow past a spherical body, the limiting value of this dimensionless number is equal to 2.

4. Dissolutions of solid body in a tubular reactor with reciprocating plate agitator

4.1 Literature survey

Numerous articles concern with the effect of vibration on mass-transfer in a gas-liquid contradicting in a reciprocating plate column (Baird & Rama Rao, 1988; Baird et al., 1992; Gomma & Al Taweel, 2005; Gomma et al., 1991; Rama Rao & Baird, 1988,2000, 2003; Sundaresan & Varma, 1990). In these papers is stated that the oscillatory motion of the gas-liquid system in reciprocating plate columns assures much higher interfacial contacting areas than in conventional bubble column with the lower power consumption. The dissolution of solid particles into water and other solutions was investigated by Tojo et al. (Tojo et al., 1981), where agitation realized by using circular flat disc without perforation. The mass-transfer coefficient is calculated by measuring the slope of the concentration time curve in the first second of particle dissolution. The breakage of chalk aggregates in both the vibrating and rotating mixers and the analyse of the model of breakage which relates the pseudo-equilibrium aggregate size to the energy dissipation rate in the stirred vessel has been investigated by Shamlou et al. (Shamlou et al., 1996). The breakage of aggregates in both the vibrating and the rotating mixers occurs by turbulent fluid stresses, but it is not depended on the source generating the liquid motion.

4.2 Experimental details

The intensification of the dissolution under the action of reciprocating agitators were carried out by means of the reactor presented by (Masiuk, 2001). It is consisted of the vertical vessel, the system measuring mass of dissolving solid body (rock-salt), the device for measuring concentration in the bulk of mixed liquid (distilled water) and the arrangement for reciprocating plate agitator at various amplitudes and frequencies. The agitation was carried out with a single reciprocating plate with flapping blades oriented horizontally where it reciprocated in a vertical direction (Masiuk[a], 1999) and different number of the multihole perforated plates agitators. The detail schemes of the vibratory mixers are given in the relevant references (Masiuk, 1996; Masiuk[b], 1999; Masiuk, 2000). Additionally, the main geometrical dimensions of mixers and the operating ranges of the process parameters are collected in the Table 3.

The reciprocating agitator was driven by the electric a.c. motor coupled through a variable gear and a V-belt transmission turned a flywheel. A vertical oscillating shaft with the perforated plates and a hardened steel ring through a sufficiently long crank shaft were articulated eccentrically to the flywheel. An inductive transducer mounted inside the ring and a tape recorder was used to measure the inductive voltage directly proportional to the total force straining of the shaft.

The average mass-transfer coefficient was calculated from a mass balance between a dissolving solid cylindrical sample and no flowing surrounding dilute solution (see equation 14). Two conductive probes connected to a multifunction computer meter were used to measuring and recording of the concentration of the achieve solution of the salt. The mass of the rock salt sample decreasing during the process of dissolution is determined by an electronic balance that connected with rocking double-arm lever. On the lever arm the sample was hanging, the other arm connected to the balance. In the present investigation the change in mass of solid body in a short time period of dissolution is very small and the mean area of dissolved cylinder of the rock salt may be used. Than the mean mass-transfer

Parameters	Operating value
Geometrical dimensions of mixer	
Vessel diameter, m	0.205
Vessel height, m	1.033
Height of liquid level in the vessel, m	0.955
Geometrical dimensions of single reciprocating plate with flapping blades	
Plate diameter, m	0.036
Width of windows in the plate, m	0.039
Plate height, m	0.036
Clearance between the plate and exhaust of the blade, m	0.015-0.024
Hydraulic diameter, m	0.00386-0.01
Geometrical dimensions of multihole perforated plates	
Agitator diameter, m	0.204
Number of plates	1-5
Diameter of hole, m	0.005-0.06
Number of holes	2-650
Distance between plates, m	0.04
Operating conditions	
Mean diameter of sample, m	0.011-0.0316
Mean length of the sample, m	0.03-0.065
Amplitude, m	0.03-0.19
Frequency, s^{-1}	0.058-1.429
Time of dissolution, min	2
Loss of mass for 2 min dissolution, kg	$0.14 \cdot 10^{-3}$-$6.83 \cdot 10^{-3}$
Mean driving force, $kg_{NaCl} \cdot (kg_{solvent})^{-1}$	0.002-0.0137

Table 3. The main geometrical dimensions of mixer and operating conditions

coefficient may be calculated from the linear kinetics equation using the mean concentration driving force of the process determined from two time response curves.

Raw rock-salt (>98% NaCl and rest traces quantitative of chloride of K, Ca, Mg and insoluble mineral impurities) cylinders were not fit directly for the experiments because their structure was not homogeneous (certain porosity). Basic requirement concerning the experiments was creating possibly homogeneous transport conditions of mass on whole interfacial surface, which was the active surface of the solid body. These requirements were met thanks to proper preparing of the sample, mounting it in the mixer and matching proper time of dissolving. As an evident effect were fast showing big pinholes on the surface of the dissolved sample as results of local non-homogeneous of material. Departure from the shape of a simple geometrical body made it impossible to take measurements of its area with sufficient precision. So it was necessary to put those samples through the process of so-called hardening. The turned cylinders had been soaked in saturated brine solution for about 15 min and than dried in a room temperature. This process was repeated four times. To help mount the sample in the mixer, a thin copper thread was glued into the sample's axis. The processing was finished with additional smoothing of the surface with fine-

grained abrasive paper. A sample prepared in this way had been keeping its shape during dissolving for about 30 min. The duration of a run was usually 30 sec. The rate of mass-transfer involved did not produce significant dimensional change in diameter of the cylinder. The time of a single dissolving cycle was chosen so that the measurement of mass loss could be made with sufficient accuracy and the decrease of dimensions would be relatively small (maximum about 0.5 mm).

Before starting every experiment, a sample which height, diameter and mass had been known was mounted in a mixer under the free surface of the mixed liquid. The reciprocating plate agitator was started, the recording of concentration changes in time, the weight showing changes in sample's mass during the process of solution, and time measuring was started simultaneously. After finishing the cycle of dissolving, the agitator was stopped, and then the loss of mass had been read on electronic scale and concentration of NaCl (electrical conductivity) in the mixer as well. This connection is given by a calibration curve, showing the dependence of the relative mass concentration of NaCl on the electrical conductivity (Rakoczy & Masiuk, 2010).

4.3 Results and discussion

In order to establish the effect of the Reynolds number on mass-transfer coefficient data obtained from the experimental investigations are graphically illustrated in a $\log\left(Sh\,Sc^{-0.33}\right)$ versus $\log(Re)$ systems for the in figure 1. These experimental results were obtained for the single reciprocating plate with flapping blades.

Figure 1 demonstrates that, within the limits of scatter among the plotted data represented by the points, the non-dimensional Sherwood number increase in the Reynolds number. The

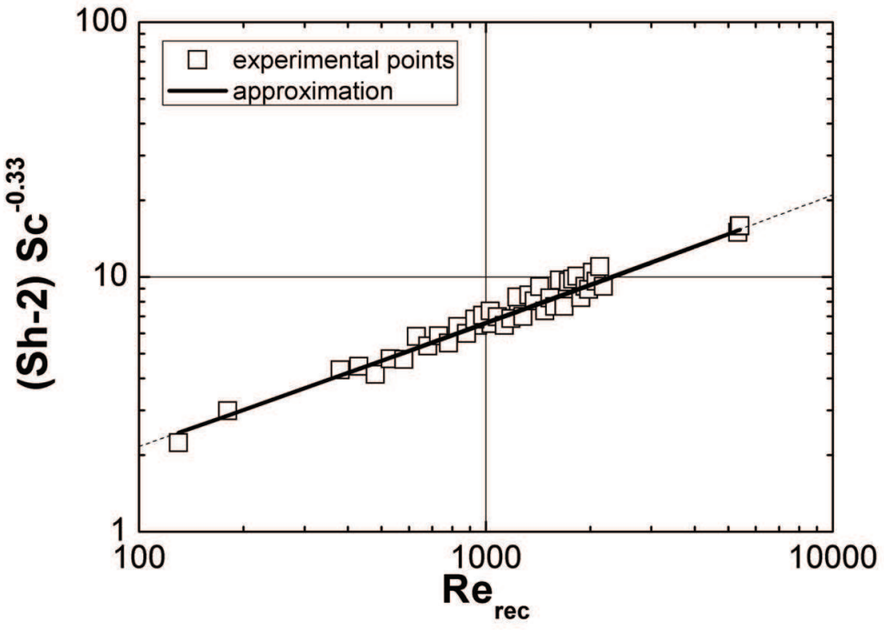

Fig. 1. Effect of the Reynolds number on the mass-transfer rate for the single reciprocating plate with flapping blades oriented horizontally

relation between the experimental results shown in this figure can be described by using the relation similar to relationship (37)

$$Sh = 0.17\, Re_{rec}^{0.33}\, Sc^{0.33}\left(1 + 0.65\, Re_{rec}^{0.22}\right) \tag{43}$$

The obtained correlation is valid for the following range of the process parameters: $Re_{rec} = 130 - 5400$; $Sc = 874 - 1244$. It is believed that the proposed dimensionless equation (44) is useful to generalize the experimental data in this work for the whole region of the reciprocating Reynolds number without the break of the correlating graphical line. Moreover, figure 1 presents a graphical form of equation (43), as the full curve, correlated the data very well with standard deviation $\sigma = 0.66$. The difference between the predicted and calculated values of the non-dimensional Sherwood number is less than $\pm 15\%$ for approximately 80% of the data points.

In present experimental investigations of the influence of the perforated plate reciprocating agitators on the mass-transfer process was additionally investigated for different number of plates varying from 1 to 5. The results of the mass-transfer experiments for different number of plates should be correlated using the relationship similar to the expression obtained for the reciprocating agitator with single perforated plate with flapping blades (equation 43).

In the present report the mass-transfer process is described by the similar somewhat modified relationship (37) between the dimensionless Sherwood number and the reciprocating Reynolds number

$$Sh = c_1\, Re_{rec}^{0.33}\, Sc^{0.33}\left(1 + c_2 Re_{rec}^{0.22}\right) \tag{44}$$

It is decided, that the constant c_2 in the relation (44) is not depended on the number of perforated plates N and equal 0.11. The constant c_1 has been computed as the function of parameter N employing the principle of least square method. Then the equation (44) for different number of the perforated plates may be rewritten in the following general dimensionless correlation

$$Sh = f^{Sh}(N)\, Re_{rec}^{0.33}\, Sc^{0.33}\left(1 + 0.11\, Re_{rec}^{0.22}\right) \tag{45}$$

where the function $f^{Sh}(N)$ is depended on the number of multihole plates.

The shape of the mass-transfer characteristics for the single plate as well as for different plates is similar and the function $f^{Sh}(N)$ may be described by means of the following relationship

$$f^{Sh}(N) = 0.17\, N \exp(-0.12\, N) \tag{46}$$

In the case of this work, the experimental data have been correlated using the new mean modified dimensionless Sherwood number, Sh^*, as a ratio of the dimensionless Sherwood, Sh, number and the dimensionless maximum density of mixing energy, $\rho^*_{E_{\max}}$.

In the selection of the suitable agitator for the transfer process, it is not sufficient to take into consideration the power consumption and mixing time separately. The density of the maximum mixing energy, $\rho_{E_{\max}}$, is defined as the product of the maximum power

consumption, $P_{\max}$, and the mixing time, t_{mix}, relate to the volume of mixed liquid, V_L (Masiuk & Rakoczy, 2007)

$$\rho_{E_{\max}} = \frac{P_{\max} t_{mix}}{V_L} \qquad [\mathrm{J \cdot m^{-3}}] \tag{47}$$

The values of the density of the maximum mixing energy (47) may be determined by using the relationships describing the maximum power consumption

$$\begin{gathered} Po = f^P(N)\, Re_{rec}^{-1}\left(1 + 0.255\, Re_{rec}^{0.95}\right) \Rightarrow \\ \Rightarrow Po = \left[0.89 N^{1.37} \exp(-0.15 N)\right] Re_{rec}^{-1}\left(1 + 0.255\, Re_{rec}^{0.95}\right) \Rightarrow \\ \Rightarrow \left(\frac{P_{\max} S^2}{\rho D^2 (2\pi A f)^3 (1 - S^2)}\right) = \left[0.89 N^{1.37} \exp(-0.15 N)\right] Re_{rec}^{-1}\left(1 + 0.255\, Re_{rec}^{0.95}\right) \end{gathered} \tag{48}$$

and the mixing time

$$\begin{gathered} \Theta = f^{t_{mix}}(N)\left(\frac{H_L}{d_h}\right) Re_{rec}^{-2}\left(1 + 0.021\, Re_{rec}^{1.25}\right) \Rightarrow \\ \Rightarrow \Theta = \left[10.5 \exp(-1.06 N)\right]\left(\frac{H_L}{d_h}\right) Re_{rec}^{-2}\left(1 + 0.021\, Re_{rec}^{1.25}\right) \Rightarrow \\ \Rightarrow \left(\frac{t_{mix}\eta}{\rho H_L^2}\right) = \left[10.5 \exp(-1.06 N)\right]\left(\frac{H_L}{d_h}\right) Re_{rec}^{-2}\left(1 + 0.021\, Re_{rec}^{1.25}\right) \end{gathered} \tag{49}$$

where: H_L - height of liquid level in the vessel, m; P - power, W; S - fraction of open area of the reciprocating plate, m; η - liquid viscosity, $\mathrm{kg \cdot m^{-1} \cdot s^{-1}}$.
The simple transformations gives the following equation describing the dimension density of the maximum mixing energy (Masiuk & Rakoczy, 2007)

$$\rho_{E_{\max}} = \psi f^E(N)\left(1 + 0.021\, Re_{rec}^{1.25}\right)\left(1 + 0.255\, Re_{rec}^{0.95}\right) \qquad [\mathrm{J \cdot m^{-3}}] \tag{50}$$

where the function $f^E(N)$ is depended on the number of the multihole plates. The parameter ψ has the following form (Masiuk & Rakoczy, 2007)

$$\psi = \frac{4\left(1 - S^2\right)}{\pi S^2} \frac{H_L^{1.15}}{d_h^{3.15}} \frac{\eta^2}{\rho} \qquad [\mathrm{J \cdot m^{-3}}] \tag{51}$$

where d_h - hydraulic diameter of perforated plate reciprocating agitators, m.
Hence, the dimensionless maximum density of maximum mixing energy, $\rho^*_{E_{\max}}$, may be calculated by means of the following equation

$$\rho^*_{E_{\max}} = \frac{\rho_{E_{\max}}}{\psi} \Rightarrow \rho^*_{E_{\max}} = f^E(N)\left(1 + 0.021\, Re_{rec}^{1.25}\right)\left(1 + 0.255\, Re_{rec}^{0.95}\right) \tag{52}$$

where:

$$f^{E}(N) = 9.35N^{1.37}\exp(-1.21N) \tag{53}$$

Taking into account the above equations (52) and (53), we find the following form of the modified dimensionless Sherwood number, Sh^*

$$Sh^* = \frac{Sh}{\rho^*_{E_{\max}}} \Rightarrow Sh^* = \frac{\left(0.17N\exp(-0.12N)\right)Re_{rec}^{0.33}\,Sc^{0.33}\left(1+0.11Re_{rec}^{0.22}\right)}{\left(9.35N^{1.37}\exp(-1.21N)\right)\left(1+0.021Re_{rec}^{1.25}\right)\left(1+0.255Re_{rec}^{0.95}\right)} \tag{54}$$

The graphical illustration of the equation (54) is given in the coordinates $\left(Sh^*Sc^{-0.33}, Re_{rec}\right)$ log-log system in figure 2.

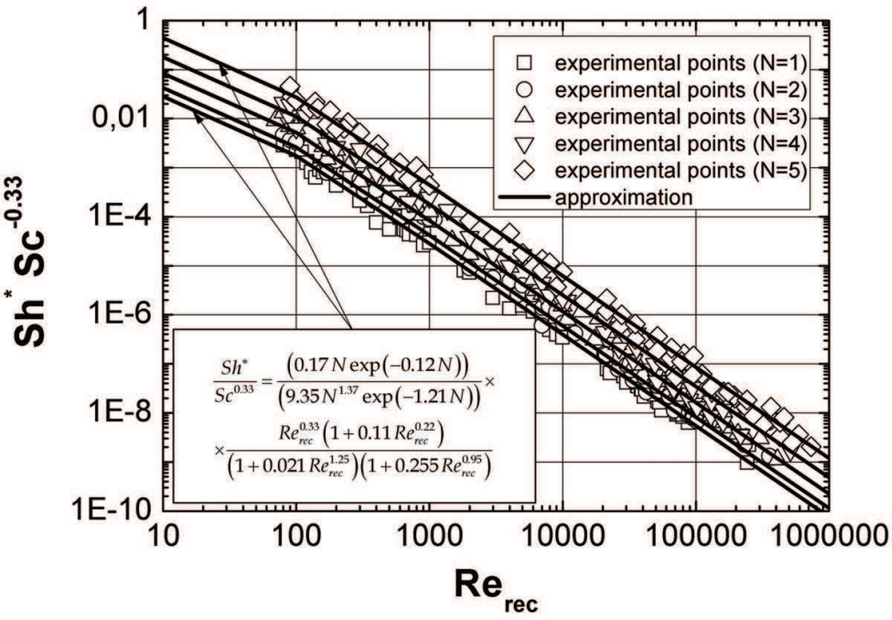

Fig. 2. Modified mass-transfer characteristics for reciprocating agitator with different number of plates

The rate of mass-transfer increases with increasing number of plates. The modified dimensionless Sherwood number, Sh^*, increases with increasing number of plates. Within the laminar region of the flow, the mass-transfer characteristics obtain the extreme (see figure 3). In the region of large Reynolds number, the curves of the modified dimensionless Sherwood number versus the reciprocating Reynolds number decreases sharply. Additionally, the change of plates of the reciprocating agitator has considerable profitable influence on the mass-transfer process.

5. Enhancement of solid dissolution process under the influence of transverse rotating magnetic field (TRMF)

The transverse rotating magnetic field (TRMF) is a versatile option for enhancing several physical and chemical processes. Studies over the recent decades were focused on application of magnetic field (MF) in different areas of engineering processes (Rakoczy &

Masiuk, 2009; Rakoczy, 2006). Static, rotating or alternating MFs might be used to augment the process intensity instead of mechanically mixing. Practical applications of RMF are presented in (Volz & Mazuruk, 1999; Melle et al., 1999; Walker et al. 2004; Nikrityuk et al. 2006; Yang et al., 2007; Fraňa et al. 2006; Spitzer, 1999).

Recently, TRMF are widely used to control different processes in the various engineering operations. This kind of magnetic field induces a time-averaged azimuthal force, which drives the flow of the electrical conducting fluid in circumferential direction. The magnetic filed lines rotate in the horizontal direction with the rotation frequency of the field, ω_{TRMF}. It is obvious that this parameter is equal to the frequency of alternating current. An electrical field, $\overline{E}$, is generated perpendicular to the magnetic field, $\overline{B}$. Perpendicular to the electric field, the Lorenz magnetic force, $\overline{F_m}$, is acting as the driving force for the liquid rotation.

The TRMF may be generated by cylindrical inductor resembling the stator of a three-phase asynchronous electrical engine. The similar inductor of TRMF was applied in (Lu & Li, 2000; Nekrassov & Chekin, 1961; Nekrassov & Chekin, 1962).

In the case of the electrical conducting fluid, the TRMF induces currents inside this liquid. These interact with the field of the inductor and generate electromagnetic force inside the electrical conducting liquid. The pattern of hydrodynamic flows due to TRMF in a cylindrical volume depends on the number of pole pair, p_{TRMF}, of TRMF inductor. The distribution of TRMF may be considered as the quasi-uniform or non-uniform for the number of pole pair equal to 1 and $p_{TRMF} > 1$, respectively. The application of TRMF may be generated the specific flow in a liquid cylindrical volume. The liquid flow is an azimuthal motion of medium around the central axis of the cylindrical volume. This flow is directed as the magnetic field rotates and the azimuthal velocity is maximal at the cylindrical vessel's walls. Obviously, this movement may determine the heat or mass-transfer inside the rotating liquid.

According to available in technical literature, research has not been focused on the mass-transfer during dissolution of a solid body to the surrounding liquid under the action of RMF. In the present report, the experimental investigations has been conducted to explain the influence of this kind of MF on the mass-transfer enhancement. Moreover, the influence of localisation of a NaCl-cylindrical sample localisation on the mass-transfer rate was experimentally determined.

5.2 Influence of transverse rotating magnetic field (TRMF) on mass-transfer process

The influence of TRMF on mass-transfer process is manifested by the magnetic force defined as the divergence of Maxwell's stress tensor and expressed by the following relation (Rakoczy & Masiuk, 2010)

$$\frac{\overline{F_m}}{V} = div\left[-\frac{1}{2}\mu_m \overline{H}^2 E + \mu_m\left(\overline{H}\overline{H}\right)\right] \Rightarrow \frac{\overline{F_m}}{V} = -\frac{1}{2\mu_m} grad\,\overline{B}^2 + \frac{1}{\mu_m} Div\left(\overline{B}\overline{B}\right) \tag{55}$$

where $\overline{B}$ - magnetic induction vector, kg·A^{-1}·s^{-1}; $\overline{H}$ - magnetic field strength vector, A·m^{-1}; V - liquid volume exposed to TRMF, m^3; μ_m - magnetic permeability, kg·m·A^{-2}·s^{-2}.

In the above equation (55), the term $\left(\frac{1}{\mu_m} Div\left(\overline{B}\overline{B}\right)\right)$ may be treated as the part of magnetic force and this expression describes the enhancement of flux density by the forced mass convection. Introducing this term in the equation (16), gives the following relationship

$$\frac{\partial c_i}{\partial \tau} + \overline{w}\, grad\, c_i - div\left(D_i\, grad\, c_i\right) + div\left(\frac{Vc_i}{\dot{G}_{TRMF}\,\mu_m} Div\left(\overline{B}\overline{B}\right)\right) = \frac{\left[\beta_i\right]_{avg}\left(grad\, c_i\right)\overline{e_r}}{\rho} \tag{56}$$

The mass flow rate for this case may be approximated by using the following relation

$$\dot{G}_{TRMF} = \rho V \omega_{TRMF} \Rightarrow \dot{G}_{TRMF} = \frac{\rho V}{\tau_{TRMF}} \tag{57}$$

where τ_{TRMF} - time of magnetic field diffusion, s.

This parameter may be defined basing on the well-known advection-diffusion type equation (Möβner & Gerbeth, 1999; Guru & Hiziroğlu, 2004)

$$\frac{\partial \overline{B}}{\partial \tau} = rot\left(\overline{w} \times \overline{B}\right) + \frac{1}{\sigma_e \mu_m} \Delta \overline{B} \tag{58}$$

where w - velocity, m·s^{-1}; σ_e - electrical conductivity, A^2·s^3·kg^{-1}·m^{-3}; $\nu_m = \left(\sigma_e \mu_m\right)^{-1}$ - effective diffusion coefficient (magnetic viscosity), m^2·s^{-1}

The above equation (58) is also called the induction equation and it characterizes the temporal evolution of the magnetic field. The term, $rot\left(\overline{w} \times \overline{B}\right)$, in this equation dominates when the conductivity is large, and can be regarded as describing freezing of MF lines into the liquid. The term, $\frac{1}{\sigma_e \mu_m} \Delta \overline{B}$, in the *B*-field equation may be treated as a diffusion term. When the electrical conductivity, σ_e, is not too large, MF lines diffuse within the fluid.

The relation (58) may be expressed as follows

$$\frac{B_0}{\tau_0}\left[\frac{\partial \overline{B}^*}{\partial \tau^*}\right] = \frac{w_0 B_0}{l_0}\left[rot^*\left(\overline{w}^* \times \overline{B}^*\right)\right] + \frac{\nu_{m_0} B_0}{l_0^2}\left[\nu_m^* \Delta^* \overline{B}^*\right] \tag{59}$$

The dimensionless form of this equation may be used to examine the effect of liquid flow on the MF distribution. The non-dimensional forms of these equations may be scaled against the term $\left(\frac{\nu_{m_0} B_0}{l_0^2}\right)$. The dimensionless form of the equation (59) may be expressed by

$$\frac{l_0^2}{\nu_{m_0} \tau_0}\left[\frac{\partial \overline{B}^*}{\partial \tau^*}\right] = \frac{w_0 l_0}{\nu_{m_0}}\left[rot^*\left(\overline{w}^* \times \overline{B}^*\right)\right] + \left[\nu_m^* \Delta^* \overline{B}^*\right] \tag{60}$$

The introduced magnetic Fourier number

$$Fo_m = \frac{\nu_{m_0} \tau_0}{l_0^2} \tag{61}$$

and magnetic Reynolds number, directly analogous to the traditional Reynolds number,

$$Re_m = \frac{w_0 l_0}{\nu_{m_0}} \tag{62}$$

describes the relative importance of advection and diffusion of the MF.
Taking into account the above definitions of the non-dimensional groups, we obtain the following general relationship of the magnetic induction equation

$$Fo_m^{-1}\left[\frac{\partial \overline{B}^*}{\partial \tau^*}\right] = Re_m\left[rot^*\left(\overline{w}^* \times \overline{B}^*\right)\right] + \left[\nu_m^* \Delta^* \overline{B}^*\right] \tag{63}$$

It should be noticed that the time of magnetic field diffusion, τ_{TRMF}, may be defined as follows

$$Fo_m^{-1} \sim 1 \Rightarrow \frac{l_0^2}{\nu_{m_0}\tau_0} \sim 1 \Rightarrow \tau_0 \sim \frac{l_0^2}{\nu_{m_0}} \Rightarrow \tau_{TRMF} = \frac{D^2}{\nu_m} \tag{64}$$

Then, the equation (57) may be rewritten in the form

$$\dot{G}_{TRMF} = \frac{\rho V}{\tau_{TRMF}} \Rightarrow \dot{G}_{TRMF} = \frac{\rho \nu_m V}{D^2} \tag{65}$$

Taking into consideration the above relations (Eqs 56 and 65), we obtain the following relationships:

$$\frac{\partial c_i}{\partial \tau} + \overline{w}\, grad\, c_i - div\left(D_i\, grad\, c_i\right) + div\left(\frac{D^2 c_i}{\rho \nu_m \mu_m} Div\left(\overline{B}\overline{B}\right)\right) = \frac{\left[\beta_i\right]_{avg}\left(grad\, c_i\right)\overline{e_r}}{\rho} \tag{66}$$

The governing equation (66) may be rewritten in a symbolic shape which is useful for the dimensionless analysis. The introduction of the non-dimensional quantities denoted by sign $\left(^*\right)$ into these relationships yield:

$$\begin{aligned} &\frac{c_{i_0}}{\tau_0}\left[\frac{\partial c_i^*}{\partial \tau^*}\right] + \frac{w_0 c_{i_0}}{l_0}\left[\overline{w}^*\, grad\, c_i^*\right] - \frac{D_{i_0} c_{i_0}}{l_0^2}\left[div^*\left(D_i^*\, grad^* c_i^*\right)\right] + \\ &+ \frac{D^2 c_{i_0} B_0^2}{\rho_0 \nu_{m_0} \mu_{m_0} l_0^2}\left[div^*\left(\frac{D^* D^* c_i^*}{\rho^* \nu_m^* \mu_m^*} Div^*\left(\overline{B}^*\overline{B}^*\right)\right)\right] = \frac{\left[\beta_i\right]_{avg_0} c_{i_0}}{l_0 \rho_0}\left[\frac{\left[\beta_i\right]_{avg}^*\left(grad^* c_i^*\right)\overline{e_r}}{\rho^*}\right] \end{aligned} \tag{67}$$

The non-dimensional forms of the above equation (67) may be scaled against the convective term $\left(\frac{w_0 c_{i_0}}{l_0}\right)$ as follows

$$\begin{aligned} &\frac{l_0}{\tau_0 w_0}\left[\frac{\partial c_i^*}{\partial \tau^*}\right] + \left[\overline{w}^*\, grad\, c_i^*\right] - \frac{D_{i_0}}{l_0 w_0}\left[div^*\left(D_i^*\, grad^* c_i^*\right)\right] + \\ &+ \frac{D B_0^2}{\rho_0 \nu_{m_0} \mu_{m_0} w_0}\left[div^*\left(\frac{D^* D^* c_i^*}{\rho^* \nu_m^* \mu_m^*} Div^*\left(\overline{B}^*\overline{B}^*\right)\right)\right] = \frac{\left[\beta_i\right]_{avg_0}}{\rho_0 w_0}\left[\frac{\left[\beta_i\right]_{avg}^*\left(grad^* c_i^*\right)\overline{e_r}}{\rho^*}\right] \end{aligned} \tag{68}$$

The equation (68) includes the following dimensionless groups characterising the influence of the TRMF on the mass-transfer process

$$\frac{DB_0^2}{\rho_0 \nu_{m_0} \mu_{m_0} w_0} \Rightarrow \left(\frac{B_0^2 \sigma_e D}{\rho_0 w_0} \right) \Rightarrow \left(\frac{B_0^2 \sigma_e}{\rho_0 \omega_{TRMF}} \right) \Rightarrow \left(\frac{B_0^2 \sigma_e D^2}{\rho_0 \nu} \right) \left(\frac{\nu}{\omega_{TRMF} D^2} \right) \Rightarrow Q\, Re_\omega^{-1} \tag{69}$$

$$\frac{[\beta_i]_{avg_0}}{\rho_0 w_0} \Rightarrow \left(\frac{[\beta_i]_{avg_0} d_s}{\rho_0 D_i} \right) \left(\frac{\nu_0}{\omega_{TRMF} D^2} \right) \left(\frac{D_i}{\nu_0} \right) \left(\frac{D}{d_s} \right) \Rightarrow Sh\, Re_\omega^{-1}\, Sc^{-1} \left(\frac{D}{d_s} \right) \tag{70}$$

Taking into account the proposed relations (29-32, 69 and 70), we find the following dimensionless governing equations

$$\begin{aligned} &S^{-1} \left[\frac{\partial c_i^*}{\partial \tau^*} \right] + \left[\overline{w}^*\, grad\, c_i^* \right] - Pe_{mass}^{-1} \left[div^* \left(D_i^*\, grad^* c_i^* \right) \right] + \\ &+ Q\, Re_\omega^{-1} \left[div^* \left(\frac{D^* D^* c_i^*}{\rho^* \nu_m^* \mu_m^*} Div^* \left(\overline{B}^* \overline{B}^* \right) \right) \right] = Sh\, Re_\omega^{-1}\, Sc^{-1} \left(\frac{D}{d_s} \right) \left[\frac{[\beta_i]_{avg}^* \left(grad^* c_i^* \right) \overline{e_r}}{\rho^*} \right] \end{aligned} \tag{71}$$

From dimensionless form of equation (71) it follows that

$$Sh\, Re_\omega^{-1}\, Sc^{-1} \left(\frac{D}{d_s} \right) \sim Q\, Re_\omega^{-1} \Rightarrow Sh \sim Q\, Sc \left(\frac{d_s}{D} \right) \tag{72}$$

The TRMF may be characterized by means of the following numbers:

- the dimensionless Chandrasekhar number

$$Q = \frac{magnetic\ force}{dissipative\ force} \Rightarrow Q = \frac{B_0^2 D \sigma_e}{\rho_0 \nu_0} \tag{73}$$

- the dimensionless field frequency based Reynolds number

$$Re_\omega = \frac{interial\ force\ /\ convection}{viscous\ force} \Rightarrow Re_\omega = \frac{\omega_{TRMF} D^2}{\nu_0} \tag{74}$$

where ω_{TRMF} - angular velocity of magnetic field, rad·s^{-1}.

The interaction between of the TRMF and the used liquid may be also described by means of the non-dimensional Hartmann number:

$$Ha = B_0 D \sqrt{\frac{\sigma_e}{\rho_0 \nu_0}} \tag{75}$$

It should be noticed that the Chandrasekhar number is the square of the Hartmann number $Q = Ha^2$. It should be noticed that the interaction between MF and the induced current in the electrically conducting liquid produces a Lorentz force:

A significant consequence of the above expressions (73-75) is that the fluid rotation under action of the TRMF may be completely characterized by means of a single dimensionless

number which is denoted as the magnetic Taylor number, Ta_m . The dimensionless Hartman and field frequency based Reynolds numbers can be unified to this non-dimensional group as follows:

$$Ta_m = \frac{centrifugal\ force}{viscous\ force} \Rightarrow Ta_m = Q\,Re_\omega \Rightarrow Ta_m = Ha^2\,Re_\omega \Rightarrow Ta_m = \frac{B_0^2 D^4 \omega_{TRMF} \sigma_e \rho_0}{\eta_0} \tag{76}$$

The above dimensionless magnetic Taylor number (76) is a measure of the azimuthal liquid velocity induced by the TRMF. Moreover, this parameter describes the Lorentz-force amplitude of RMF action and scales the force that drives the convection due to the applied TRMF.

The above definitions of non-dimensional groups (73-75) lead to the final expression of the relationship (72)

$$Sh \sim Q\,Sc\left(\frac{d_s}{D}\right) \Rightarrow Sh \sim Ha^2\,Sc\left(\frac{d_s}{D}\right) \Rightarrow Sh \sim \left(Ta_m Re_\omega^{-1}\right) Sc\left(\frac{d_s}{D}\right) \tag{78}$$

5.3 Experimental details

All experimental measurements of mass-transfer process using the TRMF were carried out in a laboratory set-up including electromagnetic field generator. A schematic of the experimental apparatus is presented in figure 3.

This setup may be divided into: a generator of the rotating electromagnetic field (1), a glass container (2) with the conductivity probes (3-4), an electric control box (5) and an inverter (6) connected with multifunctional electronic switch (8) and a personal computer (7) loaded with special software. This software made possible the electromagnetic field rotation control, recording working parameters of the generator and various state parameters.

From preliminary tests of the experimental apparatus, the glass container is not influenced by the working parameters of the stator. The TRMF was generated by a modified 3-phase stator of an induction squirrel-cage motor, parameters of which are in accordance with the Polish Standard PN-72/E-06000. The stator is supplied with a 50 Hz three-phase alternating current. The transistorized inverter (4) was used to change the frequency of the rotating magnetic field in the range of $f_{TRMF} = 1 - 50\,s^{-1}$. The stator of the electric machine, as the RMF generator is made up of a number of stampings with slots to carry the three phase winding. The number of pair poles per phase winding, p , is equal to 2. The windings are geometrically spaced 120 degrees apart. The stator and the liquid may be treated as apparent virtual electrical circuit of the closed flux of a magnetic induction. The stator windings are connected through the a.c. transistorized inverter to the power source. The generator produces an azimuthal electromagnetic force in the bulk of the TRMF reactor with the magnetic field lines rotating in the horizontal plane.

For the experimental measurements, MF is generated by coils located axially around of the cylindrical container. As mentioned above, this field is rotated around the container with the constant angular frequency, ω_{TRMF} . The TRMF strength is determined by measuring a magnetic induction. The values of the magnetic induction at different points inside the glass container are detected by using a Hall probe connected to the personal computer.

In the present work, the local mass-transfer rates were correlated with the magnetic field measurements. The aim was to investigate a dissolution process of the NaCl-cylinder probe

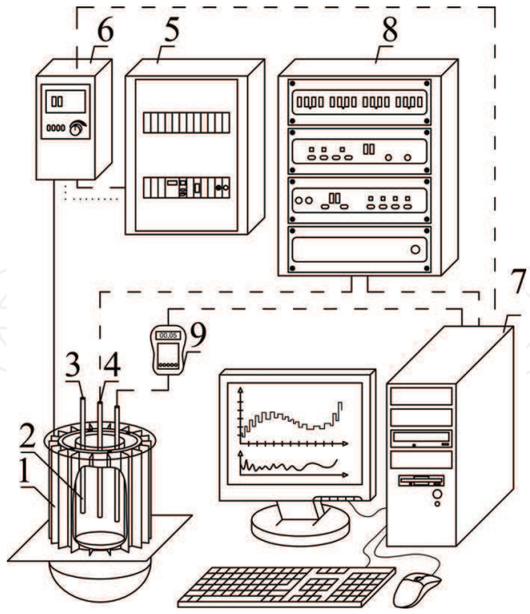

Fig. 3. Sketch of experimental set-up: 1 - generator of rotating magnetic field, 2 - glass container, 3,4 - conductivity probes, 5 - electronic control box, 6 - a.c. transistorized inverter, 7 - personal computer, 8 - multifunctional electronic switch, 9 - Hall probe

under the action of TRMF. Three measurement positions (I, II and III) were located between the wall and the centre of the glass container. All measurement positions (see Fig.4) were investigated only for a few TRMF levels. The exact localization of a NaCl cylinder sample is graphically presented in figure 4.

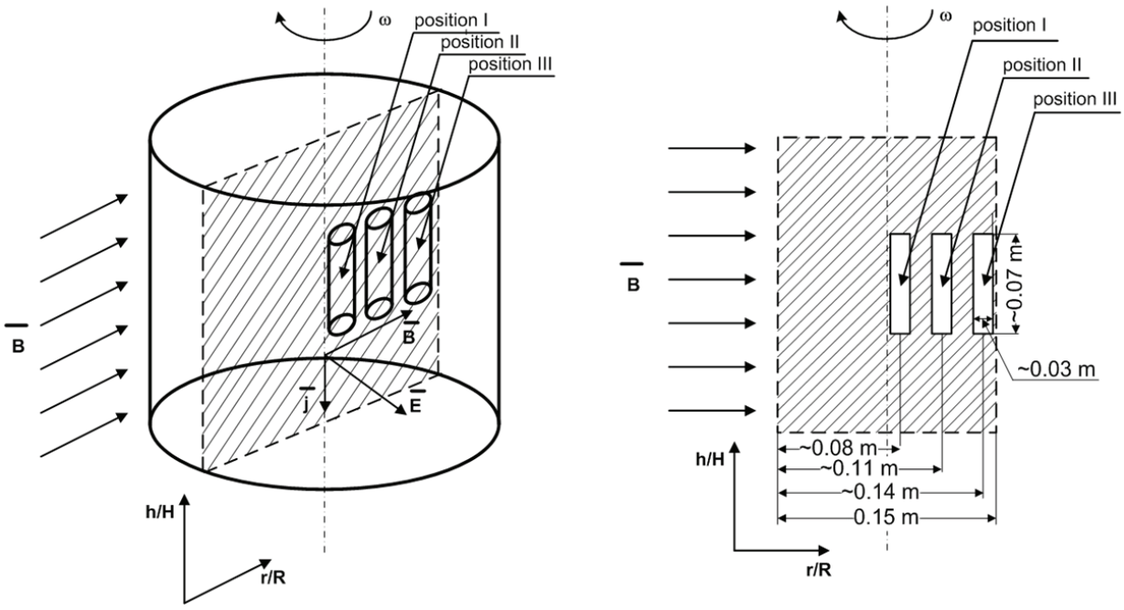

Fig. 4. The graphical presentation of measurements position inside the glass cylindrical container

The TRMF is produced by coils located around the cylinder, and the axes are directed along the radius. When the alternating current is supplied to the windings, the generated MF rotates around the cylinder column. An a.c. transistorized inverter controlled the rotating frequency (equal to the alternating frequency current in the range of $f_{TRMF} = 1 - 50 s^{-1}$).

A typical example of dependence relationship between the spatial distribution of the magnetic induction and various current values of level is presented in figure 5.

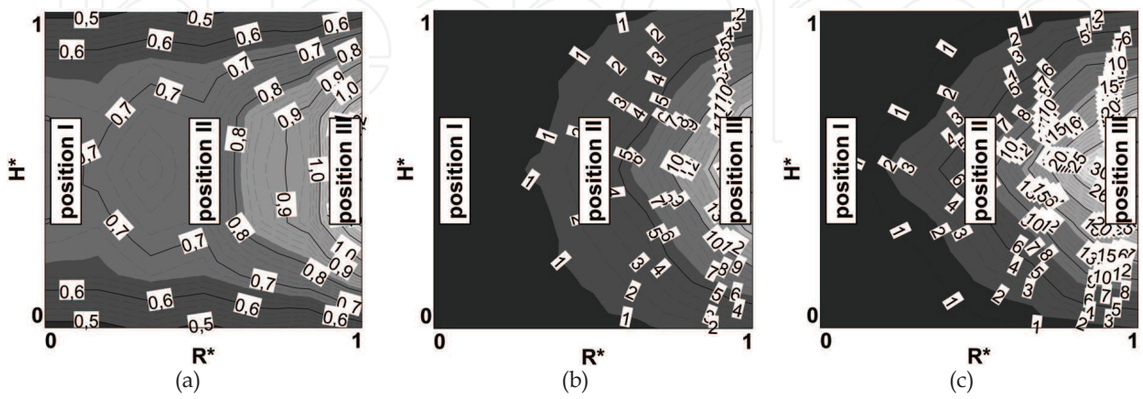

Fig. 5. The typical example of the dependence between the magnetic induction and the various values of current intensity: (a) $f_{TRMF} = 1 s^{-1}$, (b) $f_{TRMF} = 25 s^{-1}$, (c) $f_{TRMF} = 50 s^{-1}$

The TRMF with the magnetic induction, B, is controlled by using an a.c. alternating current frequency equal to the frequency of TRMF. As follows form the experimental measurements, the values of a magnetic induction are spatially distributed and time independent. It is seen that in the area occupied with this container, the TRMF distribution depends strongly on the spatial coordinates (see Fig.5). A local mass-transfer rate was

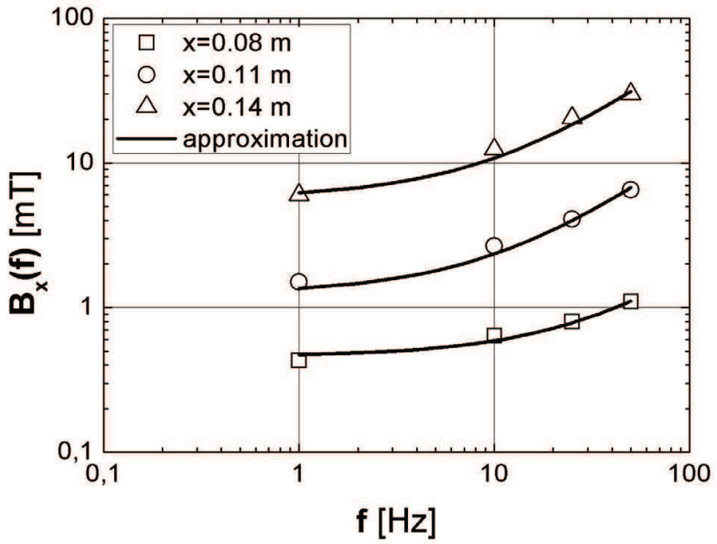

Fig. 6. The variations of the averaged magnetic induction in different localizations of NaCl-cylinder sample

obtained in three radial locations (I for x = 0.08 m; II for x = 0.11 m; III for x = 0.14 m) form the wall of the cylindrical container. It is seen that the magnetic induction at locations III and II is greater than an location I (see Fig.5). Typical profiles of the averaged magnetic induction at different locations of a NaCl-cylinder sample are graphically shown in figure 6. In order to establish the effect of a current level on the averaged values of a local magnetic induction, the obtained data shown in this figure may be analytically described by:

$$x = 0.08m \Rightarrow B_x(f) = 0.013f + 0.46 \tag{79a}$$

$$x = 0.11m \Rightarrow B_x(f) = 0.11f + 1.25 \tag{79b}$$

$$x = 0.14m \Rightarrow B_x(f) = 0.51f + 5.71 \tag{79c}$$

The enhancement of the dissolutions process under the action of TRMF was carried out by using the experimental set-up shown in Fig.3 and described in section 4.2.

5.4 Result and discussion

Under the TRMF conditions, a relationship for the mass-transfer can be described in the general form:

$$Sh = f\left[\left(Ta_m Re_\omega^{-1}\right), Sc\right] \tag{80}$$

In the presented report, the mass-transfer process under the action of TRMF is described by using the modified magnetic Taylor number, which defines the magnitude of the magnetic effect in the tested experimental set-up. The results of our experiments suggest that this non-dimensional number may be expressed as follows:

$$\left\{Ta_m\right\}_x = \frac{\left[B_x(f)\right]^2 x^4 \omega_{TRMF} \sigma_e \rho_0}{\eta_0} \tag{81}$$

The modified dimensionless field frequency based Reynolds number may defined by using the following relation

$$\left\{Re_\omega\right\}_x = \frac{\omega_{TRMF} x^2}{\nu_0} \tag{82}$$

In order to establish the effect of all important parameters on mass-transfer process in the tested set-up, in the wide range of variables data obtained in the present work have been analyzed, we propose the following relationship

$$Sh = 2 + a\left[\left\{Ta_m\right\}_x \left\{Re_\omega\right\}_x^{-1}\right]^b Sc^c \tag{83}$$

The effect of mass-transfer process under the action of RMF can be described using the variable $(Sh-2)Sc^{-c}$ proportional to the term $a\left[\left\{Ta_m\right\}_x \left\{Re_\omega\right\}_x^{-1}\right]^b$. The experimental results

obtained in this work are graphically illustrated in $\log\left\{(Sh-2)Sc^{-c}\right\}$ versus $\log\left[a\left[\left\{Ta_m\right\}_x\left\{Re_\omega\right\}_x^{-1}\right]^b\right]$ in figure 7.

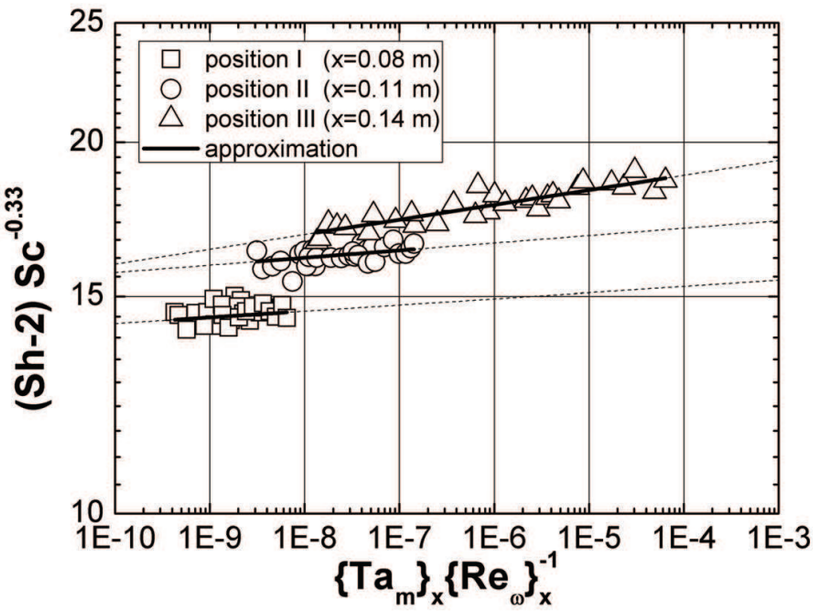

Fig. 7. The graphical presentation of mass-transfer data under the action of the TRMF

The exponent of the dimensionless Schmidt number is 0.33 as there is some theoretical and experimental evidence for this value. The experimental results in figure 7 suggest that the term $(Sh-2)Sc^{-0.33}$ versus the term $\left[\left\{Ta_m\right\}_x\left\{Re_\omega\right\}_x^{-1}\right]$ may be analytically described by a unique monotonic function. The constants and exponents are computed employing the Matlab software and the principle of least squares and the proposed relationship (19) may be rewritten in the following forms

$$x=0.08m \rightarrow \frac{(Sh-2)}{Sc^{0.33}}=16\left[\left\{Ta_m\right\}_x\left\{Re_\omega\right\}_x^{-1}\right]^{0.005} \tag{84a}$$

$$x=0.011m \rightarrow \frac{(Sh-2)}{Sc^{0.33}}=18\left[\left\{Ta_m\right\}_x\left\{Re_\omega\right\}_x^{-1}\right]^{0.006} \tag{84b}$$

$$x=0.14m \rightarrow \frac{(Sh-2)}{Sc^{0.33}}=21\left[\left\{Ta_m\right\}_x\left\{Re_\omega\right\}_x^{-1}\right]^{0.012} \tag{84c}$$

Figure 7 presents a graphical form of the above equation (84) as the full curves, correlated the experimental data very well with the standard deviation equal to $\sigma_I=0.17$ (localization I), $\sigma_{II}=0.21$ (localization II) and $\sigma_{III}=0.58$ (localization III). The average percentage errors of these data are equal to $\overline{\delta}_I=0.54\%\left(R=0.89\right)$, $\overline{\delta}_{II}=-0.18\%\left(R=0.86\right)$ and

$\overline{\delta}_{III} = 0.14\%\left(R = 0.75\right)$. Figure 7 gives an overview results, in the form of the proposed analytical description (see Eqs 84a-84c) for the experimental investigations. The first conclusion drawn from the inspection of this graph is that the proposed relationships fit the analysed experimental data very well.

Figure 7 demonstrates that, within the scatter limits among the plotted data represented by points, the dimensionless Sherwood number increases with increasing the magnetic local Taylor number. It was found that as the intensity of the MF increases, the relative velocity of liquid inside the cylindrical container increases. This liquid rotation may be defined by using the proposed term $\left[\left\{Ta_m\right\}_x \left\{Re_\omega\right\}_x^{-1}\right]$. The obtained relationships (see equation 84) indicate that the transfer rates would increase with this term for location I - $Sh \sim \left[\left\{Ta_m\right\}_x \left\{Re_\omega\right\}_x^{-1}\right]^{0.005}$, location II - $Sh \sim \left[\left\{Ta_m\right\}_x \left\{Re_\omega\right\}_x^{-1}\right]^{0.006}$ and location III - $Sh \sim \left[\left\{Ta_m\right\}_x \left\{Re_\omega\right\}_x^{-1}\right]^{0.012}$, respectively.

Moreover, the experimental results shown in figure 7 suggest the following expression:

$$\frac{\left(Sh-2\right)}{Sc^{0.33}} = fn\left[\left(\left\{Ta_m\right\}_x \left\{Re_\omega\right\}_x^{-1}\right), \left(\frac{x}{D}\right)\right] \tag{85}$$

where the Sherwood number is function of the adequate dimensionless numbers and the dimensionless location of a NaCl-cylindrical sample, $\left(\frac{x}{D}\right)$. The effect of location of sample may be described by means of the relatively simple unique dimensionless relationship as follows:

$$Sh = 2 + a\left[\left\{Ta_m\right\}_x \left\{Re_\omega\right\}_x^{-1}\right]^b Sc^c \left(\frac{x}{D}\right)^d \tag{86}$$

The constant *a* and exponent *b*, *c* and *d* in Eq.(86) are computed by using the principle of least square. Applying the software Matlab the analytical relationship may be obtained:

$$Sh = 2 + 22.5\left[\left\{Ta_m\right\}_x \left\{Re_\omega\right\}_x^{-1}\right]^{0.015} Sc^{0.33} \left(\frac{x}{D}\right)^{0.3} \tag{87}$$

The graphical presentation of Eq.(87) is given in figure 8.

The proposed form of Eq.(87), which is presented in figure 8 as the full curve, correlates the data very well with a standard deviation $\sigma = 0.05$. The average percentage error of all the data is $\overline{\delta} = -0.21\%\left(R = 0.92\right)$. Figure 8 demonstrate that, within the limits of scatter among the plotted data represented by the points, the mass-transfer rate (dimensionless Sherwood number) increase with increasing the term $a\left[\left\{Ta_m\right\}_x \left\{Re_\omega\right\}_x^{-1}\right]^b Sc^c \left(\frac{x}{D}\right)^d$. This figure shows a strongly increase in mass-transfer process when the RMF is applied. It was found that the

Sherwood number increase with increase in the local magnetic Taylor number. It should be noted that the mass-transfer rate is increased with the dimensionless location of a NaCl- cylindrical sample $\left(\frac{x}{D}\right)^{0.3}$.

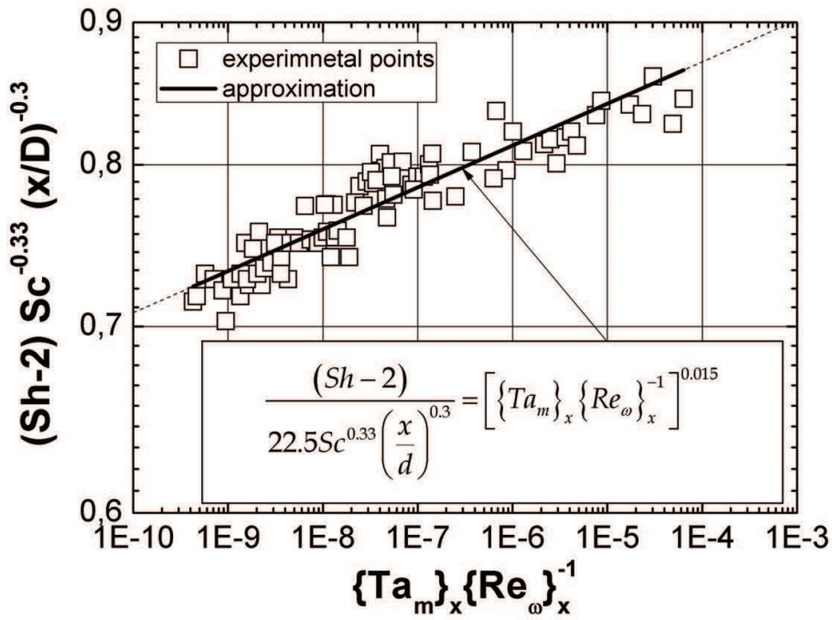

Fig. 8. The graphical presentation of equation (87)

6. Conclusion

The present considerations show interesting features concerning the effects of forced convection on the mass-transfer in the mixing systems. Based on the experimental results, the effects of the reciprocating agitators for the wide range of Reynolds number are correlated by the suitable equations. With the respect to the other very useful mass-transfer relationships given in the pertinent literature, the theoretical description of problem and the equations predicted in the present work is much more attractive because it generalizes the experimental data taking into consideration the various parameters, which defined the hydrodynamic state and the intensity of forced convection effects in the tested mixing systems. Moreover, the list of empirical equations for the prediction of mass-transfer coefficients for the rotational agitated systems has been presented. The tabulated correlations in Table 2 may be successfully applied to study the dissolution of solid bodies in the rotational stirred tank.

It should be noticed that the novel approach to the mixing process presented and based on the application of transverse rotating magnetic field (TRMF) to produce better hydrodynamic conditions in the case of the mass-transfer process. From practical point of view, the dissolution process of solid body is involved by using the turbulently agitated systems. In previous publications are not available data describing the mass-transfer operations of the dissolution process under the TRMF conditions. Therefore, the

experimental investigations have been conducted to explain the influence of this kind of magnetic field (MF) on the mass-transfer enhancement. Moreover, the influence of localization of NaCl-cylindrical sample on the mass-transfer was determined. The influence of the TRMF on this process is described using the non-dimensional parameters formulated on the base of fluid mechanics equations. These dimensionless numbers allow quantitative representation and characterization of the influence of hydrodynamic state under the TRMF conditions on the mass-transfer process. The dimensionless groups are used to establish the effect of TRMF on this operation in the form of the novel type dimensionless correlation.
The study of mass-transfer process under the action of TRMF results in significant enhancement of the solid dissolution rate. The mass-transfer measurements obtained in the presence of this kind of MF indicates a strong dependency on dissolution rate per localization of NaCl-cylindrical sample. In the present report, the mass-transfer under the action of TRMF is described by novel type of dimensionless group (the local magnetic Taylor number).

7. References

Baird, M.H.I. & Rama Rao, N.V. (1988). Characteristics of a counter current reciprocating plate bubble column. II. Axial mixing and mass transfer, *Canadian Journal of Chemical Engineering*, Vol. 66, 222-230. ISSN: 0008-4034

Baird, M.H.I., Rama Rao, N.V. & Vijayan S. (1992). Axial mixing and mass transfer in a vibrating perforated plate extraction column, *Canadian Journal of Chemical Engineering,* Vol. 70, 69-76. ISSN: 0008-4034

Barker, J.J. & Treybal, R.E. (1960). Mass transfer coefficients for solids suspended in agitated liquids, *AIChE Journal*, Vol. 6 (2), 289-295. ISSN 0001-1541

Basmadjian, D. (2004). *Mass transfer. Principles and applications*, CRC Press LLC, ISBN 0-8493-2239-1, USA.

Bird, R.B., Stewart, W.E. & Lightfoot, E.N. (1966). *Transport phenomena,* Wiley, ISBN 0-471-41077-2, USA.

Condoret, J.S., Riba, J.P. & Angelino, H. (1989). Mass transfer in a particle bed with oscillating flow, *Chemical Engineering Science,* Vol. 44, No. 10, 2107-2111. ISSN 0009-2509

Ditl, P., Rieger, F. & Roušar, I. (1991). The design of agitated dissolution tanks, *Proceedings of 7th Europ. Conf. on Mixing,* pp. 483-490, Brugge, 1991.

Fox, R.W. & McDonald A.T. (1990). *Introduction to fluid mechanics,* Wiley, ISBN 0-471-20231-2, USA.

Fraňa K., Stiller J., Grundmann R. (2006): Transitional and turbulent flows driven by a rotating magnetic field, *Magnetohydrodynamics*, Vol. 42, 187-197. ISSN 0024-998X

Garner, F.H. & Suckling, R.D. (1958). Mass transfer form a soluble solid sphere, *AIChE Journal,* Vol. 4, No. 1, 114-124. ISSN 0001-1541

Geankoplis, C.J. (2003). *Transport processes and separation processes. Principles,* Pearson Education Inc., ISBN 0-13-101367-X, USA.

Gomaa, H.G. & Al Taweel, A.M. (2005). Axial mixing in a novel pilot scale gas-liquid reciprocating plate column, *Chemical Engineering and Processing*, Vol. 44, 1285-1295. ISSN 0255-2701

Gomaa, H.G., Landau, J. & Al Taweel, A.M (1991). Gas-liquid contacting in reciprocating plate columns. I. Hydrodynamics, *Canadian Journal of Chemical Engineering,* Vol. 69, 228-239. ISSN: 0008-4034

Guru, B.S. & Hiziroğlu, H.R. (2004). *Electromagnetic field theory fundamentals,* Cambridge University Press.

Harriot, P. (1962). Mass transfer to particles: Part I. Suspended in agitated systems, *AIChE Journal,* Vol. 8, No. 93, 93-102. ISSN 0001-1541

Hartmann, H., Derksen, J.J., van der Akker, H.E.A. (2006). Numerical simulation of a dissolution process in a stirred tank reactor, *Chemical Engineering Science,* Vol. 61, 3025-3032. ISSN 0009-2509

Herdnl, G. & Mersmann, A. (1982). Fluiddynamik und Stoffübergang in gerührten Suspensionen, *Chemical Engineering and Technology,* Vol. 54, No. 3, 258-259. ISSN 1521-4125

Hixon, A. & Baum, S.J. (1941). Agitation. Mass transfer coefficients in liquid-solid agitation systems, *Industrial and Engineering Chemistry,* Vol. 33, No. 11, 1433-1438. ISSN 0888-5885

Hixon, A. & Baum, S.J. (1942). Agitation. Performance of propellers in liquid-solid systems, *Industrial and Engineering Chemistry,* Vol. 34, No. 1, 120-125. ISSN 0888-5885

Hixon, A. & Baum, S.J. (1944). Mass transfer and chemical reactions in liquid-solid agitation, *Industrial and Engineering Chemistry,* Vol. 36, No. 6, 528-531. ISSN 0888-5885

Humphrey, D.W. & Van Ness H.C. (1957). Mass transfer in a continuous-flow mixing vessels, *AIChE Journal,* Vol. 3, No. 2, 283-286. ISSN 0001-1541

Incropera, F.P. & DeWitt D.P. (1996). *Fundamentals of heat and mass transfer,* John Wiley & Sons Inc., ISBN 0-471-30460-3, USA.

Jameson, G.J. (1964). Mass (or heat) transfer form an oscillating cylinder, *Chemical Engineering Science,* Vol. 19, 793-800. ISSN 0009-2509

Kays, W.M. & Crawford M.E. (1980). *Convective heat and mass transfer,* McGraw-Hill, ISBN 0-9668461-4-1, USA.

Lemcoff, N.O. & Jameson, G.J. (1975). Solid-liquid mass transfer in a resonant bubble contractor, *Chemical Engineering Science,* Vol. 30, 363-367. ISSN 0009-2509

Lemlich R. & Levy, M.R. (1961). The effect of vibration on natural convective mass transfer. *AIChE Journal,* Vol. 7, 240-241. ISSN 0001-1541

Levins, D.M. & Glastonbury, J.R. (1972). Particle-liquid hydrodynamics and mass transfer in a stirred vessel II: Mass transfer, *Trans. Inst. Chem. Engr.*, Vol. 50, No. 32, 132-146, ISSN 0360-7275

Lu, X.S. & Li, H. (2000). Fluidization of $CaCO_3$ and Fe_2O_3 particle mixtures in a transverse rotating magnetic field, *Powder Technology*, Vol. 107, 66-78. ISSN 0032-5910

Masiuk, S. & Rakoczy, R. (2007). Power consumption, mixing time, heat and mass transfer measurements for liquid vessels that are mixed using reciprocating multiplates agitators. *Chemical Engineering and Processing,* Vol. 46, 89-98. ISSN 0255-2701

Masiuk, S. (1996). Heat transfer measurements in a liquid vessel that is mixed using vibratory agitator, *Chemical Engineering Journal,* Vol. 61, 107-112. ISSN 1385-8947

Masiuk, S. (1999)[a]. Mieszadło wibracyjne (Reciprocating agitator), Patent PL 175516.

Masiuk, S. (1999)[b]. Power consumption measurement in a liquid vessel that is mixed using vibratory agitator, *Chemical Engineering Journal,* Vol. 75, 161-165. ISSN 1385-8947

Masiuk, S. (2000). Mixing time for a reciprocating plate agitator with flapping blades, *Chemical Engineering Journal,* Vol. 79, 23-30. ISSN 1385-8947

Masiuk, S. (2001). Dissolution of solid body in a tubular reactor with reciprocating plate agitator. *Chemical Engineering Journal*, Vol. 83, 139-144. ISSN 1385-8947

Masiuk, S., Rakoczy, R. & Kordas, M. (2008). Comparison density of maximal energy for mixing process using the same agitator in rotational and reciprocating movements. *Chemical Engineering and Processing*, Vol. 47, 1252-1260. ISSN 0255-2701

Melle, S., Calderon, O.G., Fuller, G.G. & Rubio M.A. (2002): Polarizable particle aggregation under rotating magnetic fields using scattering dichroism, *Journal of Colloid and Interface Science,* Vol. 247, 200-209. DOI:10.1006/jcis.2001.8087

Möβner, R. & Gerbeth, G. (1999). Buoyant melt flows under the influence of steady and rotating magnetic fields, *Journal of Crystal Growth,* Vol. 197, 341-345. ISSN 0021-9797

Nekrassov, Z.I. & Chekin, V.V. (1961). The effect of an alternating magnetic field on a fluidized bed of ferromagnetic particles, *Izvestiya Akademii Nauk SSSR, Metallurgy Fuels,* Vol. 6, 25-29. (in Russian)

Nekrassov, Z.I. & Chekin, V.V. (1962). The effective viscosity of fluidized bed of polydisperse ferromagnetic solids in alternating magnetic field, *Izvestiya Akademii Nauk SSSR, Metallurgy Fuels,* Vol. 1, 56-59. (in Russian)

Nienow, A.W., Edwards, M.F. & Harnby, N. (1997). *Mixing in the process industries,* Butterworth-Heinemann, ISBN 0750637609, UK

Nikrityuk, P.A., Eckert, K. & Grundmann, R. (2006): A numerical study of unidirectional solidification of a binary metal alloy under influence of a rotating magnetic field, *International Journal of Heat and Mass Transfer*, Vol. 49, 1501-1515. ISSN 0017-9310

Noordsij, P. & Rotte, J.W. (1967). Mass transfer coefficients to a rotating and to a vibrating sphere. *Chemical Engineering Science,* Vol. 22, 1475-1481, ISSN 0009-2509

Rakoczy, R. & Masiuk, S. (2009). Experimental study of bubble size distribution in a liquid column exposed to a rotating magnetic field, *Chemical Engineering and Processing: Process Intensification,* Vol. 48, 1229-1240. ISSN 0255-2701

Rakoczy, R. & Masiuk, S. (2010). Influence of transverse rotating magnetic field on enhancement of solid dissolution process. *AIChE Journal,* Vol. 56, 1416-1433. ISSN 0001-1541

Rakoczy, R. (2006). Hydro-thermal behavior of liquid systems in a magnetic field, Doctro's Thesis, Szczecin University of Technology.

Rama Rao, N.V & Baird, M.H.I. (1988). Characteristics of a counter current reciprocating plate bubble column. I. Holdup, pressure drop and bubble diameter, *Canadian Journal of Chemical Engineering*, Vol. 66, 211-221. ISSN: 0008-4034

Rama Rao, N.V & Baird, M.H.I. (2000). Axial mixing and gas holdup with reciprocating doughnut plates, *Canadian Journal of Chemical Engineering*, Vol. 78, 261-264. ISSN: 0008-4034

Rama Rao, N.V & Baird, M.H.I. (2003). Gas liquid mass transfer in a 15 cm diameter reciprocating plate column, J*ournal of Chemical Technology and Biotechnology*., Vol. 78, 134-137. ISSN 1097-4660

Rousseau, R.W. (1987). *Handbook of separation process technology,* Wiley, ISBN 978-0-471-89558-9 , USA.

Shamlou, P.A., Gierczycki, A.T. & Tichner-Hooker, N.J. (1996). Breakage of flocs in liquid suspensions agitated by vibrating and rotating mixers, *Chemical Engineering Journal*, Vol. 62, 23-34. ISSN 1385-8947

Spitzer K.H. (1999): Application of rotating magnetic field in Czochralski crystal growth, *Crystal Growth and Characterization of Materials,* Vol. 38, 39-58. ISSN 0960-8974

Sugano, Y. & Rutkowsky, D.A. (1968). Effect of transverse vibration upon the rate of mass transfer for horizontal cylinder, *Chemical Engineering Science,* Vol. 23, 707-716, ISSN 0009-2509

Sundaresan, A. & Varma, Y.B.G. (1990). Interfacial area and mass transfer in gas-liquid cocurrent upflow and countercurrent flow in reciprocating plate column, *Canadian Journal of Chemical Engineering*, Vol. 68, 952-988. ISSN: 0008-4034

Tojo, K., Miyanami, K. & Minami, I. (1981). Vibartory agitation in solid-liquid mixing, *Chemical Engineering Science,* Vol. 36, 279-284. ISSN 0009-2509

Tojo, K., Miyanami, K. & Mitsui, H. (1981). Vibratory agitation in solid-liquid mixing, *Chemical Engineering Science,* Vol. 36, 279-284, ISSN 0009-2509

Treybal, R.E. (1980). *Mass transfer operations,* McGraw-Hill, ISBN 0070651760, USA

Volz, M.P. & Mazuruk, K. (1999): Thermoconvective instability in a rotating magnetic field, *International Journal of Heat and Mass Transfer,* Vol. 42, 1037-1045. ISSN 0017-9310

Walker, J.S., Volz, M.P. & Mazuruk K. (2004): Rayleigh-Bénard instability in a vertical cylinder with a rotating magnetic field, *International Journal of Heat and Mass Transfer,* Vol. 47, 1877-1887. ISSN 0017-9310

Weinspach, P.M. (1967). Der Lösevorgang im Fließbett und im Rührgefäß, *Chem.-Ing.-Tech.*, Vol. 39, No. 5/6, 213-236.

Wong, P.F.Y., Ko, N.W.M. & Yip, P.C. (1978). Mass transfer from large diameter vibrating cylinder, *Trans. Item,* Vol. 56, 214-216.

Yang, M., Ma, N., Bliss, D.F. & Bryant G.G. (2007): Melt motion during liquid-encapsulated Czochralski crystal growth in steady and rotating magnetic field, *International Journal of Heat and Mass Transfer,* Vol. 28, 768-776. ISSN 0017-9310

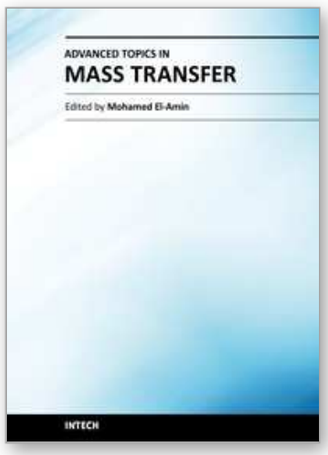

Advanced Topics in Mass Transfer

Edited by Prof. Mohamed El-Amin

ISBN 978-953-307-333-0
Hard cover, 626 pages
Publisher InTech
Published online 21, February, 2011
Published in print edition February, 2011

This book introduces a number of selected advanced topics in mass transfer phenomenon and covers its theoretical, numerical, modeling and experimental aspects. The 26 chapters of this book are divided into five parts. The first is devoted to the study of some problems of mass transfer in microchannels, turbulence, waves and plasma, while chapters regarding mass transfer with hydro-, magnetohydro- and electro- dynamics are collected in the second part. The third part deals with mass transfer in food, such as rice, cheese, fruits and vegetables, and the fourth focuses on mass transfer in some large-scale applications such as geomorphologic studies. The last part introduces several issues of combined heat and mass transfer phenomena. The book can be considered as a rich reference for researchers and engineers working in the field of mass transfer and its related topics.

InTech Europe
University Campus STeP Ri
Slavka Krautzeka 83/A
51000 Rijeka, Croatia
Phone: +385 (51) 770 447
Fax: +385 (51) 686 166
www.intechopen.com

InTech China
Unit 405, Office Block, Hotel Equatorial Shanghai
No.65, Yan An Road (West), Shanghai, 200040, China
中国上海市延安西路65号上海国际贵都大饭店办公楼405单元
Phone: +86-21-62489820
Fax: +86-21-62489821

IntechOpen